uOttawa

L'Université canadienne
Canada's university

FACULTÉ DES ÉTUDES SUPÉRIEURES ET POSTOCTORALES

uOttawa

L'Université canadienne
Canada's university

FACULTY OF GRADUATE AND POSDOCTORAL STUDIES

Marc Dilauro

AUTEUR DE LA THÈSE / AUTHOR OF THESIS

M.Sc. (Cellular and Molecular Medicine)

GRADE / DEGREE

School of Cellular and Molecular Medicine

FACULTÉ, ÉCOLE, DÉPARTEMENT / FACULTY, SCHOOL, DEPARTMENT

The Role of ACE2 and its Product, Angiotensin-(1-7), in a Model of Early Chronic Kidney Disease

TITRE DE LA THÈSE / TITLE OF THESIS

Kevin Burns

DIRECTEUR (DIRECTRICE) DE LA THÈSE / THESIS SUPERVISOR

CO-DIRECTEUR (CO-DIRECTRICE) DE LA THÈSE / THESIS CO-SUPERVISOR

EXAMINATEURS (EXAMINATRICES) DE LA THÈSE / THESIS EXAMINERS

Chris Kennedy

Leonard Kleine

Gary W. Slater

Le Doyen de la Faculté des études supérieures et postdoctorales / Dean of the Faculty of Graduate and Postdoctoral Studies

The role of ACE2 and its product, angiotensin-(1-7), in a model of early chronic kidney disease

Marc Dilauro

This thesis is submitted as a partial fulfillment of the M.Sc. program in Cellular and Molecular Medicine

June, 2009

University of Ottawa,

Ottawa, Ontario

Your file Votre référence
ISBN: 978-0-494-61157-9
Our file Notre référence
ISBN: 978-0-494-61157-9

Abstract

Angiotensin-converting enzyme 2 (ACE2) converts angiotensin II to angiotensin-(1-7) (Ang-(1-7)). The role of ACE2 and Ang-(1-7) in the progression of chronic kidney disease (CKD) is unclear. We studied the effects of ACE2 inhibition and Ang-(1-7) in the 5/6 nephrectomy (5/6 Nx) mouse model of CKD and sought to generate kidney-specific ACE2 transgenic mice. We hypothesized that pharmacological inhibition of ACE2 would accelerate kidney injury in 5/6 Nx mice whereas administration of Ang-(1-7) might be renoprotective. Four weeks after 5/6 Nx, kidney cortex ACE2 protein expression and enzymatic activity were decreased, compared to Sham-operated mice. In 5/6 Nx mice, ACE2 inhibition significantly increased urine albumin excretion, an effect reversed by Ang II AT_1 receptor antagonism. In contrast, Ang-(1-7) did not affect CKD progression. Finally, using a plasmid vector containing the human ACE2 gene linked to the nephrin promoter, transgenic mice were generated that selectively overexpress human ACE2 in the glomerular podocyte. These data suggest that kidney ACE2 is down-regulated in the 5/6 Nx mouse and that further inhibition of ACE2 increases albuminuria via an AT_1 receptor-dependent mechanism. The generation of ACE2 transgenic mice will allow for further delineation of the physiological role of ACE2 in the kidney.

Table of Contents

List of tables

List of figures

List of abbreviations

ACE	Angiotensin converting enzyme
ACE2	Angiotensin converting enzyme 2
ACEI	Angiotensin converting enzyme inhibitors
ACR	Albumin-to-creatinine ratio
α-SMA	Alpha-smooth muscle actin
Ang I	Angiotensin I
Ang II	Angiotensin II
Ang-(1-7)	Angiotensin-(1-7)
Ang-(1-9)	Angiotensin-(1-9)
ANOVA	One-way analysis of variance
ARB	Angiotensin II receptor antagonists
AT_1	Angiotensin II type I receptor
AT_2	Angiotensin II type II receptor
BP	Blood pressure
CKD	Chronic kidney disease
DMEM/F-12	Dulbecco's Modified Eagle Medium: nutrient mixture F-12
DOCA	Deoxycorticosterone acetate
DTT	Dithiothreitol
EIA	Enzyme immunoassay
ERK1/2	Extracellular signal-related kinase 1/2
ESRD	End-stage renal disease

FBS	Fetal bovine Plasma
FITC	Fluorescein isothiocyanate
GFR	Glomerular filtration rate
HA	Hemagglutinin
hACE2 ORF	Human ACE2 open reading frame
HRP	Horseradish peroxidase
MAPK	Mitogen-activated protein kinase
NP	Nephrin promoter
PBS	Phosphate buffered saline
PCR	Polymerase chain reaction
RAS	Renin-angiotensin system
RIA	Radioimmunoassay
SDS	Sodium dodecyl sulfate
S.E.M.	Standard error of the mean
SHP-1	Src-homology 2-containing protein-tyrosine phosphatase-1
SHRSP	Spontaneously hypertensive stroke-prone
STZ	Streptozotocin
TBS-T	Tris-buffered saline containing Tween 20
$TGF\beta_1$	Transforming growth factor beta 1
TFA	Trifluoroacetic acid
UUO	Unilateral ureteral obstruction
VCAM-1	Vascular cell adhesion molecule-1
5/6 Nx	5/6 nephrectomy

Acknowledgments

I would like to thank my supervisor Dr. Kevin Burns for his ongoing support, advice, and encouragement throughout my research. His expertise, understanding, and patience, added considerably to my graduate experience. I could not have been more fortunate in finding such a mentor.

In addition, I am grateful to Drs. Chris Kennedy and Hebert for serving as members of my advisory committee. I would like to thank them for their insightful comments and suggestions, as well as their guidance.

I would also like to thank Dr. Susan Robertson, Joe Zimpelmann, Anthony Carter, and Dominique Genest, whose assistance was deeply appreciated. Also, a special thanks to Dr. Chris Kennedy, Dr. Rashmi Kothary and Yves De Repentigny for their expertise in the development of our laboratory's transgenic mouse project.

I must also acknowledge the University of Ottawa (Ontario Graduate Scholarship in Science and Technology) and the Italian Night Committee (Research scholarship) for the financial assistance that I received during my graduate studies.

Lastly, I would like to express my gratitude to my family members and to all the members of the Kidney Research Centre for making my experience so enjoyable.

1.0: Introduction

1.1: Kidney structure and function

The human kidney is a complex organ that is responsible for regulating blood pressure, maintaining water and electrolyte balance, and removing metabolic waste from the body (Knepper 1997). Homeostasis is maintained in large part through the kidney's functional units known as nephrons. Each human kidney contains approximately one million nephrons. A nephron consists of a spherical filtering component, termed the renal corpuscle, and a tubule specialized for the reabsorption of water and solutes as well as the secretion of metabolic waste products from the blood into the urine.

The renal corpuscle is composed of the glomerulus and Bowman's capsule. During filtration, blood entering through the afferent arteriole is filtered by the glomerulus to produce an ultrafiltrate of renal plasma that flows into Bowman's space and then into the tubule. In the glomerulus, three major cell types are found: endothelial cells, mesangial cells, and visceral glomerular epithelial (podocytes) (Mundel and Kriz 1995). The components of the glomerulus form a molecular sieve that permits the filtration of large volumes of fluid from the capillaries into Bowman's space but restricts filtration of large plasma proteins such as albumin.

The tubule is made up of several segments, including the proximal tubule, the loop of Henle, the distal tubule, and the collecting duct (Knepper 1997). Each segment consists of a single layer of epithelial cells resting on a basement membrane. However,

the structural characteristics of these cells vary from segment to segment. Accordingly, each section has different abilities concerning water and solute transport.

In summary, the kidney is a complex organ that is responsible for maintaining important body functions such as blood pressure and fluid and electrolyte balance. Chronic kidney disease (CKD) is characterized by a significant decline in the glomerular filtration rate (GFR), which refers to the volume of plasma filtered across the glomerular capillaries per unit time (Knepper 1997). A reduced GFR can lead to impairment of the important functions that are regulated by the kidney (Gabizon, Goren et al. 1985). In this study, we investigated the progression of non-diabetic kidney disease using a specific mouse model of human chronic kidney disease CKD.

1.15: Chronic kidney disease (CKD)

In humans, CKD is defined either as kidney damage, as confirmed by kidney biopsy or markers of damage, or as the presence of decreased renal function for a period greater than 3 months (Levey, Coresh et al. 2003). The level of GFR is regarded as the best measure of overall kidney function in health and disease. The clinical syndrome of CKD is divided in terms of severity in five stages, which are based on the level of GFR. Decreased kidney function starts at a GFR below 90 ml/min/1.73 m^2 and is considered to be pronounced if the GFR is less than 60 ml/min/1.73 m^2 for more than 3 months (Indridason, Thorsteinsdottir et al. 2007). Furthermore, the presence of albumin protein in the urine, which is termed albuminuria, is widely accepted as a marker of glomerular damage (Zandi-Nejad, Eddy et al. 2004). In addition to its importance as a marker of

kidney damage, albuminuria is also an important prognostic factor for the progression of kidney disease (Remuzzi, Ruggenenti et al. 2002).

The most common risk factors for CKD include diabetes, hypertension and cardiovascular disease (Martin, Mellotte et al. 2005). Nevertheless, regardless of the primary cause of CKD, most forms of CKD with significant proteinuria (greater than 1 g/day) tend to progress to end-stage renal disease (ESRD), which is characterized by scarring of the glomeruli (glomerulosclerosis) and tubulointerstitial fibrosis, resulting in the loss of functional nephrons. The progression of CKD is also associated with activation of a hormonal system termed the renin-angiotensin system (RAS).

1.2: Renin-angiotensin system (RAS)

The systemic RAS plays a key role in blood pressure regulation, renal development and the pathogenesis of kidney disease (Kobori, Nangaku et al. 2007). The RAS consists of a series of enzymatic reactions leading to the production of angiotensin II (Ang II), a potent vasoconstrictor (**Figure 1**). Ang II is produced in two distinct steps. Firstly, a proteolytic enzyme called renin cleaves angiotensinogen, an enzyme produced in the liver, to yield angiotensin I (Ang I). The latter then undergoes further cleavage to form Ang II. This conversion is mediated by a dicarboxypeptidase known as angiotensin-converting enzyme (ACE) (Heller, Kramer et al.).

In addition to the systemic RAS, various organs in the body such as the heart, brain, liver, and kidney, possess a local intrinsic RAS (Velez 2009). The glomerular and proximal tubular components of the kidney each possess a local intrinsic RAS that

contains all the necessary enzymes for the formation of Ang II. Indeed, intrarenal concentrations of Ang II are approximately 1000-fold higher than those normally found in plasma, thus highlighting the importance of the local RAS (Seikaly, Arant et al. 1990; Siragy, Howell et al. 1995).

Ang II is a peptide hormone that acts by binding to angiotensin type 1 (AT_1) or type 2 (AT_2) receptors, both of which are classified as G protein coupled receptors (Zhuo and Li 2007). In the kidney, AT_1 receptor expression has been detected in the glomerulus, all tubular nephron segments, interstitial cells, and the renal vasculature. The signaling pathways of the AT_1 receptor include G-protein-coupled cascades leading to phospholipase C-induced stimulation of protein kinase C and of phosphoinositol turnover, leading to increased intracellular calcium concentrations (Zhuo and Li 2007). In the renal vasculature, AT_1 receptor activation stimulates vasoconstriction, whereas along the nephron, activation of AT_1 receptors increases reabsorption of Na^+ and HCO_3^- (Robey, Ruiz et al. 2002).

In contrast, AT_2 receptor expression has been detected in the adult kidney, albeit at significantly lower levels than AT_1 receptors (Ozono, Wang et al. 1997). Within the kidney, AT_2 receptors are expressed in the glomeruli, tubules, and interstitial cells. Binding of Ang II to AT_2 receptors activates cellular phosphatases, and the resulting protein dephosphorylation counteracts the activating effects of protein kinases on cell growth and other processes (Zhuo and Li 2007). Activation of AT_2 receptors is associated with enhanced sodium and water excretion (Siragy, Inagami et al. 1999). Moreover, in LLC-PK proximal tubular cells, Zimpelmann et al. reported that activation of AT_2

receptors is associated with apoptosis and inhibition of cell growth (Zimpelmann and Burns 2001).

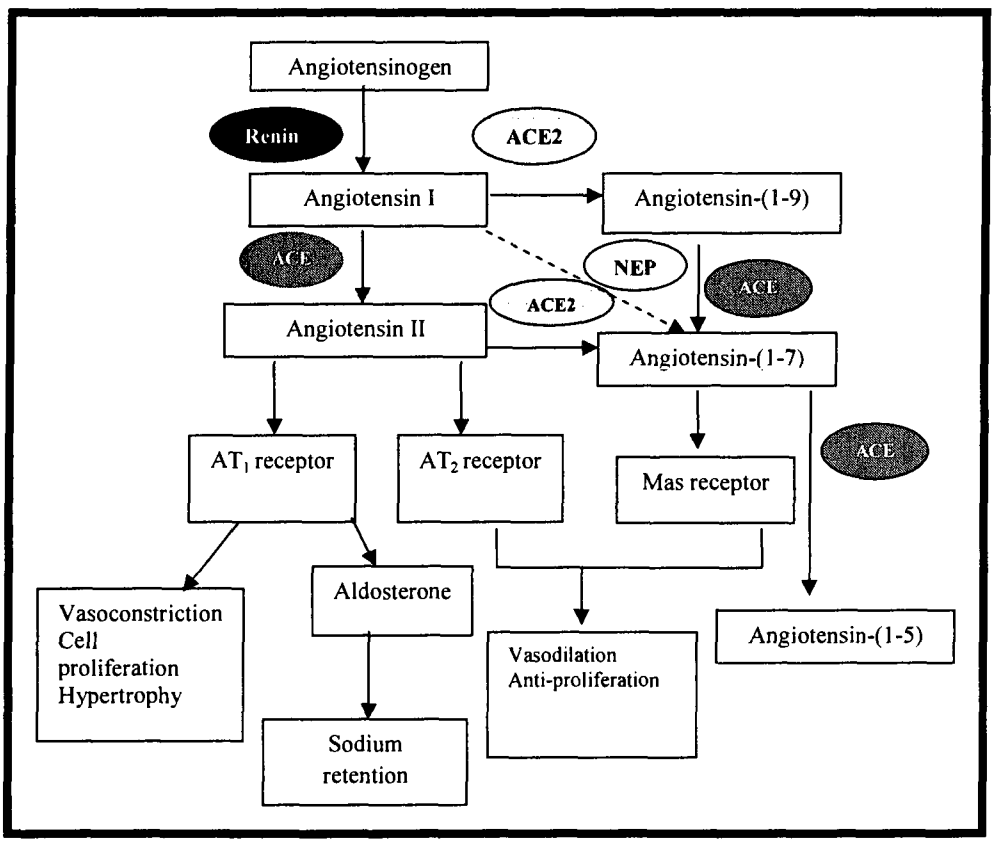

Figure 1. Schematic diagram of the metabolism of angiotensin peptides in the renin-angiotensin system (RAS).

Abbreviations: ACE: angiotensin-converting enzyme, ACE2: angiotensin-converting enzyme 2, NEP: neprilysin.

1.3: Ang II and CKD progression

Following renal injury, the RAS is activated leading to increased production of Ang II (Ruster and Wolf 2006). Ang II participates in the pathogenesis of kidney damage in several different ways. Firstly, increased levels of Ang II can cause proteinuria through both hemodynamic and nonhemodynamic mechanisms. Proteinuria is an important risk factor for the progression of CKD (Schlondorff 2008). Ang II causes efferent arteriole vasoconstriction thus, increasing glomerular capillary pressure (Wolf 1998). The increased glomerular capillary pressure in turn, causes mesangial cell hypertrophy and matrix expansion, as well as podocyte apoptosis and detachment from the glomerular basement membrane. Ang II-mediated signaling events have been shown to decrease the synthesis of key components of the glomerular filtration barrier such as negatively charged proteoglycans and nephrin transcription (Brinkkoetter, Holtgrefe et al. 2004). Therefore, Ang II negatively affects the integrity of the glomerular filtration barrier, leading to increased urinary albumin excretion.

Ang II also plays an important role in regulating inflammatory responses in the kidney during CKD (Ruiz-Ortega, Esteban et al. 2006). The recruitment of inflammatory cells into the glomerulus as well as into the tubulointerstitium plays a key role in progression of CKD. Ang II stimulates upregulation of adhesion molecules such as vascular cellular adhesion molecule-1 and integrins, allowing circulating immune cells to adhere to capillaries.

Moreover, Ang II regulates cell growth and fibrotic responses in the kidney (Ruster and Wolf 2006). Following kidney injury, Ang II stimulates proliferation of

renal cell types and induces tubular hypertrophy. Ang II also stimulates the production of extracellular matrix proteins in glomeruli.

In summary, Ang II is an important peptide hormone that is present in significant concentrations in the kidney. Ang II exerts its effects by binding predominantly to AT_1 receptors. In progressive CKD, Ang II causes several detrimental actions that enhance kidney damage and fibrosis thus impairing renal function.

1.4: Treatment of CKD

The advent of therapies that block the RAS has led to significant advances in slowing the progression of kidney disease. Experimental and clinical evidence suggest that Ang II plays a significant role in the progression of CKD (Griffin and Bidani 2006; Lee, Makaryus et al. 2009; Remuzzi, Ruggenenti et al. 2002). Pharmacological inhibition of the RAS with ACE inhibitors (ACEI) or angiotensin II receptor antagonists (ARBs) significantly reduces markers of renal injury and can even attenuate the progression of glomerular and tubulointerstitial fibrosis (Levey, Coresh et al. 2003). However, the observation that treatment with ACEI or ARBs alone does not completely inhibit the progression of CKD raises the possibility that other pathways besides the formation of Ang II may be involved in CKD progression (Remuzzi, Ruggenenti et al. 2002).

1.4: ACE2 structure and function

Angiotensin converting enzyme 2 (ACE2) was first identified in 2000 by two separate groups using distinct methodologies (Donoghue, Hsieh et al. 2000; Tipnis, Hooper et al. 2000). The ACE2 gene maps to the human X chromosome, and encodes an 805-amino acid membrane-bound glycoprotein (Tipnis, Hooper et al. 2000). Similar to ACE, ACE2 is a type I transmembrane protein comprising a short C-terminal cytoplasmic tail, a hydrophobic transmembrane region, and a heavily *N*-glycosylated N-terminal ectodomain containing the active site. However, ACE2 differs from ACE in that it functions as a monocarboxypeptidase removing a single C-terminal amino acid from its substrates, whereas ACE acts predominantly as a dicarboxypeptidase removing two C-terminal amino acids from its substrates. The active site of ACE2 is approximately 40% homologous with the catalytic domains of ACE. Of importance, the enzymatic activity of ACE2 is not blocked by conventional ACE inhibitors (Rice, Thomas et al. 2004).

ACE2 promotes the degradation of the vasoconstrictor peptide Ang II to the vasodilatory peptide angiotensin-(1-7) (Ang-(1-7)). In addition, ACE2 can convert angiotensin I (Ang I) to angiotensin-(1-9) (Ang-(1-9)), which can then be cleaved to Ang-(1-7) (**Figure 1**). However, i*n vitro* kinetic data indicate that ACE2 catalytic efficiency is ~400-fold higher with Ang II as a substrate than with Ang I (Rice, Thomas et al. 2004).

Initially, ACE2 expression was found mainly in the kidney, testis, and heart (Donoghue, Hsieh et al. 2000; Tipnis, Hooper et al. 2000). Subsequent studies showed widespread ACE2 distribution also in the lung, liver, brain, small intestine, and placenta. (Doobay, Talman et al. 2007; Hamming, Timens et al. 2004; Paizis, Tikellis et al. 2005).

1.5: ACE2 localization in the kidney

Of all the organs that ACE2 is expressed in, the kidney expresses the highest levels of ACE2 protein (Donoghue, Hsieh et al. 2000). Immunohistochemistry data indicates that ACE2 colocalizes with Ang-(1-7) to the proximal tubule (Brosnihan, Neves et al. 2003). In rat kidney, ACE2 mRNA has been detected in all nephron segments except the thick ascending limb of the loop of Henle, with relatively high levels in the proximal straight tubule (Li, Zimpelmann et al. 2005). In human kidney, ACE2 is predominantly located in the proximal tubule brush border (Lely, Hamming et al. 2004). ACE2 expression has also been observed in human renal capillary endothelium (Lely, Hamming et al. 2004).

ACE2 protein expression has also been detected in the glomerulus. Ye et al. utilized electron microscopy immunogold labeling to localize ACE2 to podocytes (Ye, Wysocki et al. 2006). Similarly, in the normal mouse glomerulus, ACE2 immunofluorescence colocalizes with podocyte and mesangial cell markers but not endothelial cell markers (Ye, Wysocki et al. 2006).

1.6: Proteolytic shedding of ACE2

In both mouse kidney and cultured polarized renal epithelial cells, ACE2 is localized primarily to the apical surface, where it can undergo proteolytic shedding. This process is mediated by tumor necrosis factor (TNF)-α-converting enzyme, and results in the release of soluble ACE2, which consists of the catalytically active ectodomain of ACE2 (Lambert, Blackburn et al. 2005; Warner, Lew et al. 2005; Ye, Wysocki et al.

2006). Indeed, ACE2 activity and protein have been detected in human urine from healthy individuals, and ACE2 activity has been measured in sheep urine and plasma (Shaltout, Westwood et al. 2007; Warner, Lew et al. 2005). The physiological role of ACE2 proteolytic shedding is unclear. However, soluble ACE2 may serve as a plasma or urinary biomarker in certain disease processes. For example, in healthy individuals, levels of circulating ACE2 are either very low or undetectable (Rice, Thomas et al. 2004). In contrast, in patients with clinical heart failure, Epelman et al. reported that soluble ACE2 activity is increased and correlates with disease severity (Epelman, Tang et al. 2008).

1.7: Phenotype of ACE2-deficient mice

The ACE2 gene knockout mouse may serve as a useful tool to establish a physiological role for ACE2 in the kidney. In the first description of the ACE2 gene knockout mouse, Crackower et al. reported that ACE2 may regulate normal cardiac function, since the dominant phenotype of these mice was defective cardiac contractility (Crackower, Sarao et al. 2002). Subsequently, Yamamoto et al. generated a distinct ACE2 knockout mouse line that exhibited normal cardiac function and morphology (Yamamoto, Ohishi et al. 2006). Similarly, Gurley et al. generated an ACE2-null mouse line in which the ACE2-deficient mice are viable, fertile, and are characterized by normal cardiac function and plasma levels of Ang II (Gurley, Allred et al. 2006). Variations in genetic background may account for the observed phenotypic differences between ACE2-null mouse lines.

Despite the observed differences in phenotype, ACE2 knockout mice can be utilized to study the effect of ACE2 gene deletion on renal physiology. For instance, Oudit et al. reported that deletion of the ACE2 gene in C57BL/6 mice caused late glomerulosclerosis and increased albuminuria (Oudit, Herzenberg et al. 2006). These effects are reversed by treatment with the AT_1 receptor antagonist irbesartan, suggesting that ACE2 deficiency causes renal injury via impaired degradation of Ang II and subsequent activation of AT_1 receptors. However, the potential independent effect of reduced Ang-(1-7) generation on renal function in the ACE2 knockout mice has not been studied.

1.8: ACE2 transgenic models

In contrast to genetic deletion of ACE2, other approaches to investigate the physiological role of ACE2 involve transgenic models with overexpression of ACE2, or gene delivery of ACE2. In the literature, three distinct ACE2 transgenic models exist. Donoghue et al. first reported sudden death due to cardiac arrhythmias in transgenic mice overexpressing ACE2 in the heart (Donoghue, Wakimoto et al. 2003). The reason for this death is unclear however, it may involve a deficiency in cardiac levels of Ang II. In contrast, in rats, lentiviral gene delivery of ACE2 significantly inhibits cardiac hypertrophy and myocardial fibrosis induced by infusion of Ang II. These data suggest that cardiac ACE2 plays an important role in preventing cardiac disease.

Rentzsch et al. generated transgenic rats (TGR(SM22ACE2)) on a spontaneously hypertensive stroke-prone (SHRSP) genetic background that expressed the human ACE2

gene in vascular smooth muscle cells (Rentzsch, Todiras et al. 2008). TGR(SM22ACE2) rats are characterized by reduced mean arterial pressure and a blunted vasoconstrictive response following intraarterial administration of Ang II, compared to SHRSP control rats. Therefore, vascular ACE2 overexpression in SHRSP rats may reduce hypertension and improve endothelial function perhaps via the ability of ACE2 to degrade Ang II to Ang-(1-7).

Despite the current transgenic and gene delivery models for ACE2, a kidney-specific ACE2 transgenic model has not been developed. Overexpression of ACE2 in the kidney could provide further insight into the role of ACE2 under normal and pathophysiologic conditions.

1.9: ACE2 and hypertension

ACE2 maps to a quantitative trait locus in the spontaneous hypertensive rat strain (SHR), and renal ACE2 expression levels are decreased in hypertension (Crackower, Sarao et al. 2002). Tikellis et al. showed that ACE2 activity and mRNA levels increased at birth in the SHR (Tikellis, Cooper et al. 2006). However, these parameters declined with the onset of hypertension as compared with control rats. These findings suggest that ACE2 is down-regulated under hypertensive conditions.

The effect of ACE2 on blood pressure regulation was investigated by Gurley et al. In contrast to the original description, ACE2 knockout mice across multiple genetic backgrounds exhibit normal cardiac function. Gurley et al. reported that infusion of Ang II to ACE2 deficient mice resulted in three-fold higher plasma levels of Ang II and almost two-fold higher blood pressures, compared with control mice (Gurley, Allred et

al. 2006). Similarly, infusion of Ang II significantly increased kidney levels of Ang II in ACE2 knockout mice, compared to wild-type control mice. These data suggest that ACE2 contributes to degradation of intrarenal Ang II *in vivo*.

1.10: ACE2 and diabetic kidney disease

Diabetic kidney disease is the most common cause of end-stage renal disease and is associated with activation of the intrarenal RAS, and increased production of intrarenal Ang II, which mediates progressive nephron injury via the promotion of growth factors, inflammatory cytokines, and glomerular and interstitial fibrosis (Hostetter, Rennke et al. 1982; Soldatos and Cooper 2008).

Substantial experimental data suggest that ACE2 is protective in diabetic kidney disease. Kidney expression of ACE2 is down-regulated in mouse models of diabetes and in diabetic patients (Mizuiri, Hemmi et al. 2008; Reich, Oudit et al. 2008; Tikellis, Johnston et al. 2003; Ye, Wysocki et al. 2004; Ye, Wysocki et al. 2006). Pharmacological inhibition of ACE2 in streptozotocin (STZ)-induced diabetic mice increases albuminuria and glomerular extracellular matrix expansion (Soler, Wysocki et al. 2007). These effects are associated with increased ACE expression in glomeruli and renal vessels. Thus, in diabetic kidney disease, the combination of increased ACE expression and inhibition of ACE2 could increase levels of Ang II, leading to accelerated glomerular injury. Similarly, Wong *et al.* showed that ACE2-deficient mice exhibit accelerated diabetic renal injury (Wong, Oudit et al. 2007). ACE2 knockout mice were crossed with Akita mice, a model of type I diabetes mellitus. Diabetic ACE2 knockout mice ($Ace2^{-/y}Ins2^{WT/C96Y}$) exhibit increased albuminuria, mesangial matrix scores and

glomerular basement membrane thickening compared to diabetic control mice. Treatment of diabetic ACE2 knockout mice with the AT_1 receptor antagonist irbesartan reduced albuminuria. Therefore, a deficiency in renal ACE2 activity may accelerate diabetic kidney injury via impaired degradation of Ang II and increased activation of AT_1 receptors.

In summary, ACE2 is expressed at high levels in the kidney particularly in the proximal tubule, a segment that contains all the components of the RAS. ACE2 may play an important role as a counter-regulatory enzyme to ACE in that it degrades Ang II to Ang-(1–7). There is increasing evidence that ACE2 may be involved in disease states such as diabetic kidney disease and hypertension. However, there remains much to learn about ACE2 in the kidney, including its regulation in normal and pathophysiologic states and the biological effects of its product, Ang-(1-7).

1.11: Formation of intrarenal Ang-(1-7)

Ang-(1-7) is generated in the vascular endothelium from the precursor Ang I or by the degradation of Ang II (Santos, Brosnihan et al. 1992). Endothelial production of Ang-(1-7) may contribute to circulating levels, and indeed, under physiological conditions plasma concentrations of Ang-(1-7) are in the picomolar range, comparable to the plasma levels of Ang II (Joyner, Neves et al. 2007; Pendergrass, Averill et al. 2006; Pendergrass, Pirro et al. 2008).

Similarly, Ang-(1-7) is also formed in the kidney from either Ang I or Ang II (Stephenson and Kenny 1987; Trask and Ferrario 2007). Intrarenal levels of Ang-(1-7) are relatively high and comparable to levels of Ang II (Joyner, Neves et al. 2007). In

Sprague-Dawley rats, Ang-(1-7) and Ang II are present at ~300 and ~800 fmol /g kidney tissue, respectively (Joyner, Neves et al. 2007).

Substantial evidence suggests that ACE2 is the predominant enzyme involved in the generation of intrarenal Ang-(1-7). Li et al. demonstrated in isolated rat proximal tubular segments, that Ang-(1-7) is generated from Ang I in an ACE2-dependent manner (Li, Zimpelmann et al. 2005). However, incubation with Ang II or luminal perfusion of Ang II did not result in the generation of Ang-(1-7) (Li, Zimpelmann et al. 2005). In contrast, studies in rat kidney cortex and isolated sheep proximal tubules have shown that Ang-(1-7) is primarily generated via the ACE2-dependent degradation of Ang II (Shaltout, Westwood et al. 2007; Tikellis, Johnston et al. 2003). Despite the discrepancies between these studies, it is clear that ACE2 plays an important role in promoting the formation of Ang-(1-7) in the kidney.

1.12: Kidney receptors for Ang-(1-7)

Once formed, intrarenal Ang-(1-7) exerts its signaling effects by binding primarily to the G protein-coupled Mas receptor. The Mas gene was discovered in 1986 and was originally described as a protooncogene due to its ability to transform NIH 3T3 cells (Young, Waitches et al. 1986). In the mouse, deletion of the Mas gene abolishes the intrarenal binding and functional responses to Ang-(1-7) (Santos, Simoes e Silva et al. 2003). Subsequent radioligand binding studies have confirmed that Mas binds Ang-(1-7) with high affinity (Santos, Simoes e Silva et al. 2003). Ang-(1-7) may also bind to AT_1 and AT_2 receptors however, these interactions are considered low affinity (Santos,

Campagnole-Santos et al. 1994). Therefore, the physiological effects of Ang-(1-7) may be mediated by Mas and angiotensin receptors.

1.13: Localization of Mas in the kidney

By immunocytochemistry, Chappell et al. showed that Mas receptor protein is expressed in the mouse afferent arteriole and in tubular epithelium, primarily on the apical surface (Chappell, Modrall et al. 2004). Similarly, Mas protein expression has been detected in cultured human proximal tubular cells and mesangial cells by immunoblot (Zimpelmann and Burns 2009). Using reverse transcription polymerase chain reaction, Su et al. reported abundant levels of Mas mRNA in rat renal cortex and in primary cultures of rat proximal tubular cells (Su, Zimpelmann et al. 2006).

1.14: Regulation of renal hemodynamics by Ang-(1-7)

In the non-renal vasculature, Ang-(1-7) exerts a vasodilatory effect that involves increased production of nitric oxide, prostaglandins, or endothelium-dependent hyperpolarizing relaxing factor (Dilauro and Burns 2009). In contrast, the role of Ang-(1-7) in the regulation of renal hemodynamics is unclear, and data are conflicting (Benter, Ferrario et al. 1995; Dharmani, Mustafa et al. 2007; Sampaio, Nascimento et al. 2003; van der Wouden, Ochodnicky et al. 2006). The renal hemodynamic effects of Ang-(1-7) are difficult to assess *in vivo* since renal blood flow is regulated by numerous vasoconstrictor and vasodilator influences (Navar, Inscho et al. 1996). Therefore, it is

possible that the hemodynamic effects of Ang-(1-7) on the renal vasculature may be masked *in vivo*.

1.15: Intrarenal Ang-(1-7) and cell growth pathways

Studies performed by our laboratory suggest that Ang-(1-7) may regulate cell growth in the kidney (Dilauro and Burns 2009). In rat proximal tubular cells, Su et al. showed that Ang-(1-7) inhibits Ang II-stimulated phosphorylation of mitogen-activated protein kinases (MAPK), an effect that is reversed by the Mas receptor antagonist A-779 (Su, Zimpelmann et al. 2006). In renal epithelial LLC-PK cells, Gava et al. demonstrated that Ang-(1-7) binds the Mas receptor and blocks high glucose-stimulated phosphorylation of p38 MAPK, an effect that is associated with activation of Src-homology 2-containing protein-tyrosine phosphatase-1 (SHP-1) (Gava, Samad-Zadeh et al. 2009). Ang-(1-7) also inhibits high glucose-stimulated cell protein synthesis, and prevents the stimulatory effect of glucose on TGF-β1. These findings are consistent with the reported growth inhibitory properties of Ang-(1-7) on cardiac tissue. For instance, in a rat deoxycorticosterone acetate (DOCA)-salt model of hypertension, infusion of Ang-(1-7) prevented myocardial and perivascular fibrosis by inhibiting collagen deposition (Grobe, Mecca et al. 2006).

In contrast, Ang-(1-7) stimulates growth of mesangial cells. Zimpelmann and Burns showed that Ang-(1-7) increased MAPK phosphorylation in cultured human mesangial cells, associated with stimulation of DNA synthesis, arachidonic acid release, and production of transforming growth factor-beta 1 (TGF-β1) and extracellular matrix

proteins (Zimpelmann and Burns 2009). These cells were shown to express the Mas receptor, and the growth stimulatory effects of Ang-(1-7) were inhibited by the Mas receptor antagonist A-779, but not by AT_1 or AT_2 receptor antagonism, and were dependent on upstream activation of p38 MAPK. These data suggest that binding of Ang-(1-7) to the Mas receptor stimulates mesangial cell growth responses.

Taken together, these data suggest that in proximal tubule, Ang-(1-7) exhibits growth inhibitory effects and antagonizes the effects of Ang II and high glucose, whereas in mesangial cells, it appears to stimulate cell growth pathways. The overall effect of Ang-(1-7) on kidney cell growth and function is unclear and awaits further studies, including those directed at other glomerular cells and tubular segments.

1.16: Renal phenotype of Mas deficient mice

The effect of genetic deletion of the Mas receptor on renal physiology has been investigated by two separate groups. Pinheiro et al. reported that C57BL/6 Mas knockout mice exhibit a renal phenotype characterized by sodium and water retention, glomerular hyperfiltration, microalbuminuria, and renal fibrosis (Pinheiro, Ferreira et al. 2009). This phenotype is also associated with upregulation of renal AT_1 receptors. Therefore, it is possible that the effects of Mas receptor deficiency may at least partly be due to increased AT_1 receptor signaling activity, in addition to loss of Ang-(1-7) action. In contrast, Esteban et al. reported that C57BL/6 mice with Mas gene deletion had attenuated renal injury in the unilateral ureteral obstruction (UUO) and renal ischemia/reperfusion (I/R) models of renal injury (Esteban, Heringer-Walther et al. 2009). Thus, Mas deficiency

resulted in inhibition of NF-κB activation and reduced levels of cytokines, suggesting that blockade of Mas signaling events may prevent renal inflammation. Taken together, these data are conflicting in that the Pinheiro et al. study supports a renoprotective role for Ang-(1-7) whereas the study by Esteban et al. suggests that Ang-(1-7) could exacerbate renal injury by promoting inflammation in the kidney.

1.17: Ang-(1-7) and diabetic kidney disease

Benter et al. first reported a renoprotective role for Ang-(1-7) in the development of diabetic kidney disease (Benter, Yousif et al. 2007; Benter, Yousif et al. 2008). Administration of Ang-(1-7) to STZ-induced diabetic male rats reduced proteinuria and restored vascular reactivity in isolated renal artery segments (Benter, Yousif et al. 2007). Similarly, treatment of STZ-induced diabetic SHR with Ang-(1-7) attenuated NAPDH oxidase activation, diminished proteinuria and decreased the diabetes-induced increase in renal vascular responsiveness to endothelin-1, norepinephrine, and Ang II (Benter, Yousif et al. 2008).

In contrast, Shao et al. showed that chronic infusion of Ang-(1-7) to STZ-diabetic male rats accelerates renal injury (Shao, He et al. 2008). Ang-(1-7) increased proteinuria as well as TGF-β1 mRNA and protein levels in the diabetic kidney, when compared to untreated diabetic rats. It is possible that differences in rodent strain and age as well as the dose of Ang-(1-7) and length of treatment could contribute to the discrepancies between these studies. Moreover, the cell-specific signaling pathways associated with Ang-(1-7) in the kidney could play a role in this variable response.

1.18: 5/6 nephrectomy (5/6 Nx) model of CKD

The 5/6 nephrectomy (5/6 Nx) model of CKD is frequently utilized to study the progression of renal disease (Kren and Hostetter 1999). This model involves removal of one kidney and either partial infarction or amputation of two thirds of the other kidney. This model has been applied mainly to different strains of rats, although it has also been employed in mice, dogs, and rabbits (Eddy, Falk et al. 1986; Gabizon, Goren et al. 1985; Robertson, Goldschmidt et al. 1986). Importantly, this model shares several features observed in human CKD namely, activation of RAS, hypertension, proteinuria, and glomerulosclerosis (Kren and Hostetter 1999).

1.19: Summary

In summary, the kidney is a complex organ that is responsible for regulating important physiological functions such as blood pressure and fluid and electrolyte balance. Progressive CKD is characterized by a significant decline in GFR and is associated with activation of the RAS, leading to the production of the vasoconstrictor peptide Ang II. Significant proteinuria is also associated with progressive CKD. The pathogenesis of CKD involves Ang II, which causes detrimental effects in the kidney by binding to AT_1 receptors. ACE2 is highly expressed in the kidney and may serve as a counter-regulatory enzyme to ACE by degrading Ang II to Ang-(1-7). Animal studies suggest that ACE2 and possibly its product, Ang-(1-7), are protective in diabetic kidney disease. In models of non-diabetic chronic kidney disease, however, the role of ACE2 as

a protective factor has not been studied, nor has the possible contribution of the ACE2 product, Ang-(1-7).

1.20: Rationale

ACE2 is highly expressed in the kidney, where it plays a key role in degrading Ang II to form Ang-(1-7). Studies using ACE2 inhibitors and knockout mice suggest that the actions of ACE2 are critical in certain disease states such as diabetic kidney disease and hypertension. However, the role of ACE2 in the progression of non-diabetic CKD remains unexplored. Moreover, the association between renal disease and intrarenal levels of Ang-(1-7) is not fully understood. Therefore, we sought to investigate the role ACE2, and its product, Ang-(1-7), in a model of CKD called the 5/6 nephrectomy (5/6 Nx) mouse model. Further understanding of the role of ACE2, and its product, Ang-(1-7), in the progression of CKD may provide novel therapeutic options for this disease.

The generation of a kidney-specific ACE2 transgenic mouse may provide further insight into the role of ACE2 in normal and pathophysiologic states. Currently, however, no model exists in which ACE2 is overexpressed specifically within the kidney. The podocyte is a highly specialized cell type of the glomerulus that plays a key role in regulating the glomerular filtration barrier. Podocyte dysfunction plays an essential role in the development of proteinuria and glomerulosclerosis that occurs during progressive CKD. Therefore, we sought to generate ACE2 transgenic mice that selectively overexpress ACE2 in the podocyte cells of the kidney. These mice would be utilized in future studies in order to investigate the effect of ACE2 overexpression in the 5/6 Nx model.

1.21: Objectives

The major purpose of this study was to determine the role of ACE2 and its product, Ang-(1-7), in preventing progressive renal injury in a model of CKD, the 5/6 Nx.

The specific objectives are as follows:

1) To study the effect of 5/6 Nx on renal expression of ACE2 and ACE, as well as intrarenal levels of Ang II and Ang-(1-7).
2) To determine if ACE2 inhibition accelerates renal injury in 5/6 Nx mice.
3) To determine if ACE2 inhibition enhances signaling associated with renal AT_1 receptors.
4) To investigate the potential role of Ang-(1-7) as a renal protective agent in 5/6 Nx mice.
5) To determine if Ang-(1-7) in combination with the AT_1 receptor blocker losartan will attenuate the progression of CKD to greater extent than either monotherapy.
6) To generate ACE2 transgenic mice which overexpress the human ACE2 gene in a podocyte-specific manner.

1.22: Hypothesis

I hypothesized that ACE2 inhibition would accelerate kidney injury in 5/6 Nx mice whereas administration of Ang-(1-7) to 5/6 Nx mice would cause a renoprotective effect.

2.0: Statement of Contributions

I have performed all the experiments and assays described in this thesis except for the following:

1) All 5/6 Nx surgical procedures were performed by Anthony Carter (laboratory technician). I was present during all of surgical procedures and I assisted Anthony with various tasks such as preparing the mice for surgery and sterilizing the surgical equipment.
2) Histologic analyses were performed under the supervision of Dr. Susan Roberston (renal pathologist). Dominique Genest (undergraduate summer student) also assisted with the histologic analyses.
3) For the experiments involving Sham mice treated with MLN-4760 (MLN), measurements of blood pressure, urinary albumin excretion, and FITC-inulin clearance were performed by Dominique Genest under my supervision.
4) Plasma electrolytes were analyzed by Gaby Cherton-Horvat (laboratory manager).
5) Microinjection of the ACE2 transgene into mouse embryos was performed by Yves De Repentigny (laboratory technician for Dr. Kothary).

3.0: Materials and Methods

3.1: Experimental groups

Male FVB/NJ mice, at 5 weeks of age, were obtained from Charles Rivers Laboratories (Wilmington, MA). All mice were housed in the Animal Care Facility at the University of Ottawa with free access to food and water. The experimental protocols were approved by the University of Ottawa Animal Care and Use Committee.

The mice were randomly divided into 7 experimental groups, with 12 mice in each group:

1. Sham-operated mice (Sham)

2. Vehicle-treated 5/6 nephrectomized mice (5/6 Nx) (with water-filled osmotic mini-pump (Alzet model 1004, Alza Corp. Palo Alto, Ca))

3. 5/6 Nx mice treated with the AT_1 receptor antagonist losartan (Merck Research Laboratories, Rhway, NJ) (5/6 Nx+Los: 25 mg/kg/day via osmotic minipump)

4. 5/6 Nx mice treated with the ACE2 antagonist, MLN-4760 (Millennium Pharmaceuticals, Boston, MA) (5/6 Nx+MLN: 80 mg/kg/every 2 days by subcutaneous injection) (Wong, Oudit et al. 2007)

5. 5/6 Nx mice treated with both losartan and MLN (5/6Nx+MLN+Los)

6. 5/6 Nx mice treated with Ang-(1-7) (Bachem Bioscience, King of Prussia, PA) (5/6 Nx+Ang-(1-7): 24 μg/kg/hr via osmotic minipump) (Menon, Soto-Pantoja et al. 2007)

7. 5/6 Nx mice treated with Ang-(1-7) in combination with losartan (5/6 Nx+Ang-(1-7)+Los.)

3.2: 5/6 Nx surgical procedure

Mice were subjected to either sham surgery or two-step 5/6 Nx under halothane anesthesia. During the first session, a dorsal longitudinal incision was made and the right kidney was exposed. Surgical ablation of the upper and lower poles of the right kidney was performed by cautery to remove 2/3 of the right kidney. One week after the first session, a dorsal longitudinal incision was made and the left kidney was exposed and then removed to induce a total 5/6 Nx. Sham mice underwent identical surgical procedures. However the right and left kidneys were simply manipulated. The osmotic mini-pumps were implanted following completion of the second session of the 5/6 Nx. In the appropriate groups, subcutaneous injections of MLN commenced the day after the second session of the 5/6 Nx was completed. Injections of MLN continued until the end point of the study was reached.

3.3: Tissue preparation

The mice were euthanized at four weeks post 5/6 Nx (age 13 weeks). Eight out of the 12 mice in each group were anesthetized using isoflurane and then euthanized by cardiac puncture. The remnant kidney was perfused with ice-cold phosphate buffered saline (PBS) to flush any remaining blood. Next, the remnant kidney was quickly removed, weighed and bisected longitudinally, with one half for histological analysis and the other for immunoblot analyses. Kidney mass index was determined as the ratio of the weight of the remnant kidney divided by body weight. Pieces of cortex from the bisected remnant kidney were dissected and snap frozen in liquid nitrogen and then stored at -

80°C for later measurement of ACE2 activity and immunoblot analysis of ACE2, ACE, TGFβ1, vascular cell adhesion molecule-1 (VCAM-1), alpha-smooth muscle actin (α-SMA), and p38 and extracellular signal-regulated kinases 1 and 2 (ERK1/2) mitogen-activated protein kinases (MAPK). The remaining 4 mice from each group were utilized for FITC-inulin clearance measurements after which these mice were then killed by CO_2 narcosis followed by decapitation. The remnant kidney from each mouse was removed, weighed and snap frozen in liquid nitrogen and stored at -80°C for later measurement of whole kidney levels of Ang II and Ang-(1-7). Similarly, plasma samples were collected from each mouse for the measurement of Ang II and Ang-(1-7). The following parameters were measured on all 12 mice per group: body weight, remnant kidney weight, systolic blood pressure, urinary albumin excretion, and Plasma analysis of Na^+, Cl^-, Ca^{2+}, PO_4^{2-}, urea, and HCO_3^-.

3.4: Blood pressure measurements

Systolic blood pressure (BP) was measured by tail-cuff plethysmography (BP-2000; Visitech Systems, Apex, NC). Mice were trained for an initial period of five consecutive days, and baseline measurements were subsequently collected for an additional five days. Systolic BP was then measured at four weeks post 5/6 Nx.

3.5: Measurement of glomerular filtration rate (GFR) in conscious mice

Kidney function of 5/6 Nx and sham mice was evaluated by determination of GFR, using fluorescein isothiocyanate (FITC)-inulin clearance (Qi and Breyer 2009). FITC-inulin (5%) (Sigma-Aldrich) was dissolved in 0.9% sodium chloride by heating the solution in boiling water. To remove residual FITC not bound to inulin, the solution was dialyzed in 1 L of 0.9% NaCl at room temperature for 24 hours using a 1,000-Da cutoff dialysis membrane (Spectra/Pro 6, Spectrum Laboratories, Rancho Dominguez, CA). The dialysis bottle was wrapped with aluminum foil. Before use, the dialyzed FITC-inulin solution was sterilized by filtration through a 0.22-μm filter (Costar, Corning, NY).

The mice were restrained inside 50 mL centrifuge tubes with large air-holes drilled in the tip and the sterilized FITC-inulin (3.74 μl/g body weight) was injected by tail vein. Approximately 30 μl of blood was collected via the saphenous vein at 3, 5, 7, 10, 15, 35, 55, and 75 min postinjection of FITC-inulin, yielding 15 μl of plasma for the determination of FITC concentration by fluorescence. Since pH significantly affects FITC fluorescence values, plasma samples were buffered to pH 7.4, by mixing 10 μl of plasma with 90 μl of 0.5 M HEPES (pH 7.4). Titrated samples were then loaded onto a 96-well plate, 100 μl sample/well. Plasma fluorescence was determined at each time point using a FLUOstar Galaxy fluorescence microplate reader (BMG Labtechnologies Inc., Durham, NC) at an excitation wavelength of 485-nm and an emission wavelength of 538-nm. The decay in plasma fluorescence levels was fit to a two-phase exponential decay curve using nonlinear regression (GraphPad Prism; GraphPad Software, San Diego, CA). GFR was calculated using the equation: $GFR = I/(A/\alpha + B/\beta)$, where I is the

amount of FITC-inulin delivered by tail vein injection; A and α are the y-intercept and the decay constant of the rapid (initial) decay phase, respectively; and B and β are the y-intercept and the decay constant of the slow decay phase, respectively. GFR values were corrected for body weight and expressed as μl of FITC-inulin cleared per minute per gram body weight (μl/min/g BW).

3.6: Albuminuria, Plasma analysis, and hematocrit measurements

Urinary excretion of albumin was determined using the albumin-to-creatinine ratio (ACR) on morning spot urine collections. Urinary albumin and creatinine levels were determined using ELISA (Albuwell M; Exocell Inc., Philadelphia, PA) and creatinine assay kit (Creatinine Companion; Exocell Inc.), respectively.

Blood samples for plasma analysis were collected by cardiac puncture using a heparinized syringe. The blood was then transferred to ice-cold eppendorf tubes, and then centrifuged at 3, 000 *g* for 10 minutes at 4°C. Plasma electrolytes (Na^+, Cl^-, Ca^{2+}, PO_4^{-2}, HCO_3^-) and plasma levels of urea were assayed using the Synchron CX5 Delta (Beckman Coulter, Inc., Fullerton, CA).

In addition, a small portion (~20 μl) of the blood from each cardiac puncture was collected in heparinized micro-hematocrit capillary tubes (Baxter, Deerfield, IL) for hematocrit measurements. The capillaries were spun at 2,000 *g* for 5 minutes at room temperature. Hematocrit measurements were then performed using a micro-hematocrit capillary tube reader (Critocaps, Oxford Lab., Baxter, Deerfield, IL).

3.7: Histopathology

Remnant kidneys were resected immediately after blood collection and sectioned longitudinally. The sections of remnant kidney were incubated overnight in 10% paraformaldehyde, subsequently dehydrated, and paraffin-embedded. Sections were cut at 3 μm thickness, stained with Sirius red, which stains for collagen type IV. The sections were then assessed for glomerular diameter and relative mesangial area. The glomeruli in each section were measured using an ocular grid micrometer at 400X magnification. Approximately 25-30 glomeruli were examined per section. For the determination of relative mesangial area, high-resolution digital photographs of 25-30 glomeruli sectioned through, or close to, the hilum were prepared from the Sirius red-stained sections from each mouse. These photographs were subsequently quantified by assessment of the ratio of surface area of mesangium to total glomerular surface area with color-assisted image analysis using ImagePro software (version 5.1, Bethesda, MD). Each section was examined by a kidney pathologist (Dr. Susan Robertson) in a blinded manner with regard to treatment groups.

3.8: ACE2 activity assay

Kidney cortex samples were homogenized or lysed, respectively, in a buffer consisting of 50 mM HEPES, pH 7.4, 150 mM NaCl, 0.5% Triton X-100, 0.025 mM $ZnCl_2$, and 1.0 mM PMSF and then clarified by centrifugation at 12, 000 *g* for 15 minutes at 4^0C. To prevent undesirable hydrolysis of the substrate by a range of nonmetalloprotease enzymes, an EDTA-free inhibitor cocktail tablet (Roche,

Indianapolis, IN) was added to the lysis buffer prior to homogenization or cell lysis. Kidney cortex ACE2 activity was determined following incubation with the intramolecularly quenched synthetic ACE2-specific substrate *o*-amino-benzoic acid-Ser-Pro-Tyr(NO_2)-OH (Peptides International, Inc., Louisville, KY). Briefly, 5 µl of cortex homogenate or cell lysate was added to a well of a black flat-bottom 96-well plate containing 95 µl of 100 mM Tris pH 6.5, 1.5 mM NaCl, 1 mM PMSF, 1 mM N-ethylmaleimide, 2 µg bovine serum albumin (BSA), and 33 µM substrate. Each assay was performed in quadruplicate (1.0 µM MLN-4760 (Millennium Pharmaceuticals) was added to two of the wells in addition to the components previously mentioned in order to inhibit ACE2 enzymatic activity). After incubation at room temperature for 4 hours, fluorescence was measured using the FLUOstar Galaxy fluorescence microplate reader (BMG Labtechnologies, Inc.) at an excitation wavelength of 320-nm and an emission wavelength of 420-nm. Blank values were substracted from all fluorescence values. Fluorescence resulting from ACE2 specific activity was determined by subtracting the values obtained in the presence of MLN-4760 from the values obtained in the absence of MLN-4760. ACE2 specific fluorescence values were then corrected for protein content (in tissue homogenate and cell lysate samples). Purified mouse recombinant ACE2 (R&D Systems, Minneapolis, MN) was used to calibrate activity, and results were expressed as nanogram equivalents per microgram protein.

Similar experiments were performed to measure ACE2 enzymatic activity using transfected COS-7 cell lysates. In the case of the COS-7 cells, the lysates were sonicated for 2 seconds prior to centrifugation.

3.9: Immunoblotting

The following protocol was used for all immunoblotting experiments in this thesis. A list of antibodies used can be found in the appendix (Table 4). Kidney cortex tissue was homogenized in a buffer consisting of 62.5 mM Tris-HCl (pH 6.8), 2% w/v sodium dodecyl sulfate, 10% glycerol, 50 mM dithiothreitol (DTT), and 0.1% w/v bromophenol blue. The lysate was then boiled for 5 minutes, followed by centrifugation at 12, 000 *g* for 5 minutes to remove insoluble debris. The protein concentration of the supernatant was quantified using the Bradford reagent method (Bio-Rad Laboratories, Mississauga, ON, Canada). Equal amounts of protein lysates (20 μg) were run on 10-15% sodium dodecyl sulfate (SDS)-polyacrylamide gels and transferred to nitrocellulose membranes (Bio-Rad). The membranes were blocked with 5% skim milk in Tris-buffered saline (pH 7.6) containing 0.1% Tween 20 (TBS-T) for 1 hour at room temperature. The membranes were incubated overnight at 4°C with a primary antibody. After incubation with primary antibodies, the membranes were briefly washed with TBS-T and then incubated with their respective secondary antibodies (**Appendix: Table 5**) for 1 hour at room temperature and then washed for 90 minutes in TBS-T. Proteins were detected by enhanced chemiluminescence (ECL; GE Health Care Bio-Sciences, Baie d'Urfe, Quebec, Canada). Prestained standards were used as molecular weight markers (Bio-Rad). To control for protein loading, all membranes were stripped with Pierce IgG elution buffer (Pierce, Rockford, IL) and reprobed with either an antibody to β-actin or the corresponding antibody that recognizes both the phosphorylated and unphosphorylated forms of the protein of interest. Densitometric analysis of the protein

bands was performed using the Kodak 1D Image Analysis software (Eastman Kodak Company, Rochester, NY).

Immunoblot experiments to detect human ACE2 protein expression were also performed using transfected COS-7 cell lysates. In the case of the COS-7 cells, the lysates were sonicated for 2 seconds prior to centrifugation.

3.10: Kidney and plasma levels of Ang II and Ang-(1-7)

Whole kidney and plasma levels of Ang II were measured using a peptide radioimmunoassay kit (RIA) (Sampaio, Souza dos Santos et al.) that contains an Ang II selective polyclonal antibody and ^{125}I-Ang II (Peninsula Laboratories, LLC., San Carlos, CA). Whole kidney and plasma levels of Ang-(1-7) were measured using a peptide enzyme immunoassay (EIA) kit that contains an Ang-(1-7) selective polyclonal antibody (Peninsula Laboratories). For both assays, the manufacturer's instructions were followed.

Before analysis, whole kidney samples were homogenized in 1 mL ice-cold methanol in the presence of protease inhibitors (50 mM EDTA, 0.5 mM *o*-phenanthroline, 1 mM N-ethylmaleimide, and 0.1 mM pepstatin A. Samples were then centrifuged at 25, 000 *g* for 10 minutes at 4°C. In order to remove the methanol that would prevent the angiotensin peptides from absorbing to the C18 Sep-columns, the supernatants from the kidney homogenates were dried in a vacuum centrifuge (Savant, Hicksville, NY). The dried residue was reconstituted in 4 mL of 50 mM sodium phosphate buffer (pH 7.4), containing 0.1% BSA and then divided into two equal fractions (one for kidney levels of Ang II and the other for kidney levels of Ang-(1-7)).

Angiotensin peptides were extracted from each fraction using C18 Sep-columns (Waters Corporation, Milford, MA), as described below.

Blood samples were collected in eppendorf tubes kept on ice containing 0.01 mM p-hydroxy-mercury benzoate, 1.5 mM o-phenanthroline, 0.01 mM PMSF, 0.05 mM pepstatin A, and 10 mM EDTA, and then centrifuged at 3, 000 *g* for 20 minutes at 4°C. The plasma samples were extracted by first acidifying the plasma using an equal volume of 1% trifluoroacetic acid (TFA) in order to remove interfering proteins such as albumin. Next, the samples were centrifuged at 25, 000 *g* for 10 minutes at 4°C. The supernatants were transferred to new tubes, each containing 4 mL of 50 mM sodium phosphate buffer (pH 7.4) with 0.1% BSA. Each sample was then divided into two equal fractions (one for plasma levels of Ang II and the other for plasma levels of Ang-(1-7)), which were stored at -80°C until further processing.

The extraction of angiotensin peptides was performed as follows. The C18 Sep-columns (Waters Corporation, Milford, MA) were equilibrated with 1 mL of a buffer consisting of 60% acetonitrile, 1% TFA, and 39% distilled water followed by three washed (3 mL) with 1% TFA. After sample application, each C18 Sep-column was washed twice with 3 mL of 1% TFA. The Ang peptides were eluted in a polyprolyene tube with 2 × 1 mL of the same buffer that was used to equilibrate the columns. Eluants were concentrated to dryness using a vacuum centrifuge and then stored at -80°C until the RIA and EIA were performed.

3.11: Generation and genotypic analysis of transgenic mice

An 8.3-kb fragment of the murine nephrin promoter (NP) (a kind gift from Dr. Kennedy's laboratory), which included the 5' untranslated and 5' flanking regions of the murine NPHSI gene was cloned immediately upstream of the human ACE2 open reading frame (hACE2 ORF) (GI: 194306626). The hACE2 ORF contained a double 5' hemagglutinin (2XHA) epitope tag. The NP-2XHA-hACE2 transgene was linearized with *Hin*dIII/RsrII and then microinjected into FC1F1 (FVB/CD-1) mouse embryos at a concentration of 2.0 ng/μl and incubated overnight to assure viability. Embryos were then surgically transferred to the oviduct of pseudo-pregnant CD-1 recipient female mice. Both the embryo donor mice and the recipient mice were purchased from Charles River Laboratories, Inc. (Wilmington, MA).

Genomic DNA was extracted from tail snips of the resulting pups (founders) using the Extract-N-Amp Tissue PCR kit (Sigma-Aldrich, St. Louis, MO). Isolated DNA samples were used directly for genotyping by polymerase chain reaction (PCR). The PCR conditions were as follows: 94 °C 2 min, 30 cycles of 94 °C 15 sec, 60 °C 30 sec, 68 °C 30 sec, and an extension step of 7 min at 72 °C. The primers used were: forward primer, 5'-CAGGGAAGACAGCAACAAACAAG-3' and reverse primer, 5'-GAGAAGGAGCCAGGAAGAGCTT-3'. Afterwards, the PCR products were separated by electrophoresis on a 1.5% agarose gel containing ethidium bromide and then visualized under ultraviolet light. Transgenic mice were differentiated from wild-type by the presence or absence of the expected band at 125 base pairs, respectively.

3.12: Transfection of COS-7 cells

In order to determine if the ACE2 transgene yielded functional human ACE2 protein, transfection experiments using COS-7 cells were performed. COS-7 cells (ATCC) (CRL-1651) were cultured in Dulbecco's Modified Eagle Medium: nutrient mixture F-12 (DMEM/F-12) supplemented with 5% fetal bovine Plasma (FBS) and 1% penicillin/streptomycin. The cells were maintained in a 37°C incubator containing a 5% CO_2-95% air mixture. Once the cells reached 60-70% confluence, they were transfected with either 2XHA-hACE2 or the empty PCDNA3 vector using the PolyFect Transfection Reagent (QIAGEN Inc., Mississauga, ON, Canada) according to the manufacturer's instructions.

Protein lysates from untransfected COS-7 cells and COS-7 cells transfected with either the empty PCDNA3 vector, or 2X-HA-hACE2 were resolved by SDS-PAGE. The resulting immunoblot was probed with a specific antibody against human ACE2 (**Appendix: Table 5**) and then stripped with Pierce IgG elution buffer (Pierce) and reprobed with an HA tag specific antibody (**Appendix: Table 5**). The immunoblot was also probed with a β-actin specific antibody to verify equal protein loading.

Protein lysates from untransfected COS-7 cells and COS-7 cells transfected with either the empty PCDNA3 vector, or 2X-HA-hACE2 were isolated and incubated with a specific ACE2 fluorogenic substrate in the presence or absence of 1.0 μM MLN in order to measure ACE2 enzymatic activity (*refer to 2.6: ACE2 activity*).

3.13: Statistical analyses

Data were analyzed using GraphPad Prism (GraphPad Software version 4.02, San Diego, CA). Values are reported as means ± standard error of the mean (S.E.M.). Statistical comparisons were made using either Student's *t* test or one-way analysis of variance (ANOVA) followed by Tukey's multiple comparison test. A p-value less than 0.05 was considered statistically significant.

4.0: Results

4.1: Body weights, kidney weights, plasma analysis and hematocrit measurements

At baseline before treatments, body weights were comparable amongst groups of mice (**Table 1**). Similarly, at four weeks post 5/6 Nx, no significant differences were observed between the groups of mice in terms of body weight. The remnant kidney weights were similar between treatment groups of 5/6 Nx mice. More importantly, 5/6 Nx is associated with significant hypertrophy since the mean remnant kidney weight from each of the 5/6 Nx treatment groups was comparable to mean kidney weight from Sham mice.

Plasma analysis at four weeks post 5/6 Nx revealed similar concentrations of Na^+, Cl^-, Ca^{2+}, PO_4^{2-}, and HCO_3^- between Sham and 5/6 Nx mice (**Table 2**). Furthermore, treatment of 5/6 Nx mice with either losartan, MLN, or Ang-(1-7) did not affect the plasma concentrations of the previously mentioned analytes. In contrast, plasma urea concentrations were significantly increased in 5/6 Nx mice, compared to Sham mice. However, urea concentrations did not significantly differ between treatment groups of 5/6 Nx mice. Potassium concentrations were omitted from **Table 2** since the samples were hemolyzed. Following hemolysis, potassium values are abnormally elevated and thus, they are not reliable (Hawkins 2003).

At four weeks post 5/6 Nx, hematocrit measurements were significantly decreased in 5/6 Nx mice, compared to Sham mice (**Table 3**). No significant differences were observed between treatment groups of 5/6 Nx mice in terms of hematocrit values.

Table 1. Body weights, remnant kidney weights and their ratios.

	Baseline	4 weeks post 5/6 Nx		
Group[a]	BW (g)	BW (g)	RKW (g)[b]	RKW/BW ratio (kg/g)
Sham	25.0 ± 0.4	26.7 ± 0.6	0.1794 ± 0.003	6.78 ± 0.21
5/6 Nx	25.2 ± 0.5	27.4 ± 0.6	0.1776 ± 0.006	6.58 ± 0.21
5/6 Nx+Los	25.5 ± 0.4	27.0 ± 0.4	0.1809 ± 0.009	7.05 ± 0.19
5/6 Nx+MLN	25.6 ± 0.4	26.4 ± 0.5	0.1755 ± 0.006	6.60 ± 0.20
5/6 Nx+MLN+Los	24.6 ± 0.6	26.0 ± 0.4	0.1755 ± 0.005	6.72 ± 0.22
5/6 Nx+Ang-(1-7)	24.4 ± 0.4	25.8 ± 0.7	0.1793 ± 0.005	6.98 ± 0.17
5/6 Nx+Ang-(1-7)+Los	25.9 ± 0.4	27.8 ± 0.5	0.1765 ± 0.015	7.06 ± 0.18

Abbreviations: BW: body weight, RKW: remnant kidney weight, RKW/BW: remnant kidney-to-body weight ratio, Los: losartan (AT_1 receptor antagonist), MLN: MLN-4760 (specific inhibitor of ACE2). The abbreviations for losartan and MLN-4760 were used in all subsequent tables and figures.

Data are means ± standard errors

Data compared using one-way ANOVA followed by Tukey's post-hoc test

[a] All groups were n=12 except for 5/6 Nx+MLN+Los (n=11)

[b] For Sham mice, the entire right kidney was weighed.

Table 2. Plasma analysis at four weeks post 5/6 Nx.

Group[a]	Na^+ (mM)	Cl^- (mM)	Ca^{2+} (mM)	PO_4^{2-} (mM)	Urea (mM)	HCO_3^- (mM)
Sham	147.1 ± 0.7	114.3 ± 1.0	2.10 ± 0.05	2.68 ± 0.18	7.5 ± 1.3	17.9 ± 1.3
5/6 Nx	148.3 ± 1.3	114.4 ± 1.0	2.13 ± 0.06	2.43 ± 0.20	17.4 ± 0.6 *	19.3 ± 0.8
5/6 Nx+MLN	145.5 ± 0.7	114.0 ± 2.2	2.10 ± 0.05	2.21 ± 0.17	15.6 ± 1.5 *	19.2 ± 0.5
5/6 Nx+Los	149.0 ± 0.7	113.3 ± 1.4	2.05 ± 0.03	2.27 ± 0.12	17.8 ± 1.4 *	17.7 ± 0.6
5/6 Nx+MLN+Los	152.8 ± 4.2	114.8 ± 2.1	2.01 ± 0.05	2.13 ± 0.21	22.3 ± 3.4 *	16.3 ± 0.6
5/6 Nx+Ang-(1-7)	148.4 ± 0.7	113.7 ± 2.4	2.12 ± 0.04	2.26 ± 0.12	18.1 ± 1.6 *	17.3 ± 0.5
5/6 Nx+Ang-(1-7)+Los	148.4 ± 0.8	115.1 ± 2.5	2.14 ± 0.05	2.27 ± 0.11	18.1 ± 1.2 *	18.0 ± 1.0

Data are means ± standard errors

Data compared using one-way ANOVA followed by Tukey's post-hoc test

* $P < 0.05$ vs. Sham

[a] All groups were n=8 except for 5/6 Nx+MLN+Los (n=7)

Table 3. Hematocrit measurements at four weeks post 5/6 Nx.

Group[a]	Hematocrit (%)
Sham	41.7 ± 0.6
5/6 Nx	32.8 ± 0.5 *
5/6 Nx+MLN	33.7 ± 0.5 *
5/6 Nx+Los	34.1 ± 0.7 *
5/6 Nx+MLN+Los	32.5 ± 0.5 *
5/6 Nx+Ang-(1-7)	32.2 ± 0.6 *
5/6 Nx+Ang-(1-7)+Los	33.1 ± 0.8 *

Data are means ± standard errors [a] All groups were n=12 except for 5/6Nx+MLN+Los. which was n=11

Data compared using one-way ANOVA followed by Tukey's post-hoc test

* $P < 0.05$ vs. Sham[b] Hematocrit is expressed as the percentage of the total blood volume occupied by the red blood cells

[c] Data are means ± standard errors

[d] Data compared using one-way ANOVA followed by Tukey's post-hoc test

[e] * $P < 0.05$ vs. Sham

[a] All groups were n=8 except for 5/6Nx+MLN+Los. (n=7)

4.2: Effect of ACE2 inhibition, losartan treatment, and Ang-(1-7) on systolic blood pressure

Systolic blood pressure measurements were performed to determine the effect of ACE2 inhibition, losartan treatment, and administration of Ang-(1-7) on blood pressure values in 5/6 Nx mice. At baseline before treatments, blood pressures were similar between all groups of mice (**Figure 2**). Four weeks after 5/6 Nx, there was a modest increase in blood pressure in 5/6 Nx mice, compared to Sham mice (**Figure 2**). However, this increase did not reach statistical significance. Treatment of 5/6 Nx mice with losartan significantly decreased blood pressure values. In contrast, treatment of 5/6 Nx mice with either MLN, or Ang-(1-7) did not affect blood pressure values. Combination therapy of MLN and losartan caused a modest decrease in blood pressure that was not statistically different than blood pressure values of vehicle-treated 5/6 Nx mice or 5/6 Nx mice treated with losartan. In contrast, combination therapy of losartan and Ang-(1-7) significantly decreased blood pressure, compared to either vehicle-treated 5/6 Nx mice or 5/6 Nx mice treated with Ang-(1-7).

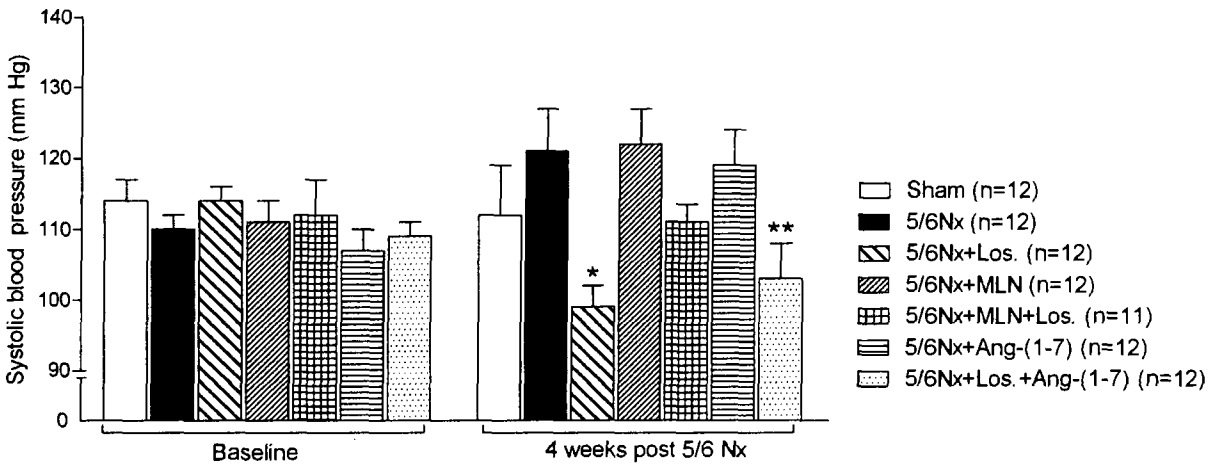

Figure 2. Systolic blood pressure measurements at baseline and four weeks post 5/6 Nx.

Systolic blood pressure measurements were performed by tail-cuff plethysmography. Values are means ± S.E.M. Statistical comparisons were made using one-way ANOVA followed by Tukey's post-hoc test. * $P < 0.05$ vs. 5/6 Nx (at 4 weeks), ** $P < 0.05$ vs. 5/6 Nx+Ang-(1-7) (at 4 weeks), and vs. 5/6 Nx (at 4 weeks).

4.3: Decreased FITC-inulin clearance in 5/6 Nx mice

In order to assess the kidney function of the different groups of mice, the FITC-inulin clearance method, which provides an estimate of the glomerular filtration rate (Qi and Breyer 2009), was used.

At four weeks, FITC-inulin clearance values for Sham mice were consistent with published values from age-matched wild-type FVB/NJ mice (Qi, Fujita et al. 2005). 5/6 Nx was associated with an approximate ~50% reduction in FITC-inulin clearance, compared to Sham mice (**Figure 3**). No significant differences were observed between 5/6 Nx treatment groups in terms of FITC-inulin clearance values.

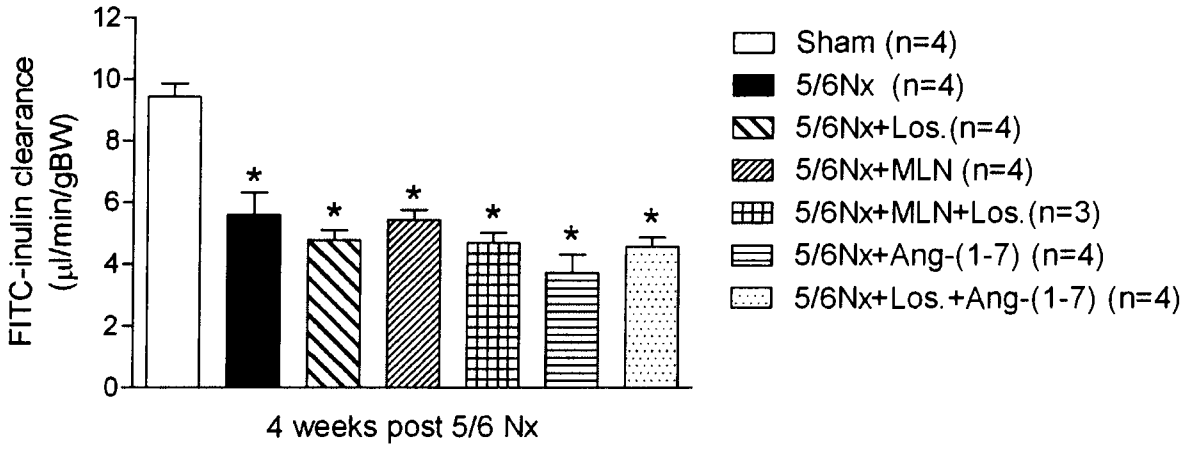

Figure 3. FITC-inulin clearance at four weeks post 5/6 Nx.

Kidney function was assessed using the FITC-inulin clearance method. Values are means ± S.E.M. Statistical comparisons were made using one-way ANOVA followed by Tukey's post-hoc test. * $P < 0.05$ vs. Sham.

4.4: Kidney histological analyses

To determine if treatment of 5/6 Nx mice with MLN worsened histologic measures of kidney injury, sections of remnant kidney tissue at four weeks post 5/6 Nx, were stained with Sirius red, and then used for measurements of relative mesangial area and glomerular diameter. The histological findings are summarized in **Table 4**.

Relative mesangial area signifies the percentage of total glomerular area that consists of mesangium. 5/6 Nx was associated with a modest but not significant increase in relative mesangial area, compared to Sham mice. In contrast, treatment of 5/6 Nx mice with Ang-(1-7) caused a significant increase in relative mesangial area, compared to Sham mice. Furthermore, 5/6 Nx was associated with a modest but not significant increase in glomerular diameter, compared to Sham mice. Although Ang-(1-7) increased relative mesangial area, it did not however, affect glomerular diameter in 5/6 Nx mice. Treatment of 5/6 Nx mice with either losartan or MLN did not significantly affect relative mesangial area or glomerular diameter, compared to vehicle-treated 5/6 Nx mice.

Table 4. Histologic analyses at four weeks post 5/6 Nx.

Group[a]	Relative mesangial area (%)	Glomerular diameter (μm)
Sham	9.7 ± 3.1	65 ± 1.4
5/6 Nx	14.0 ± 1.4	70 ± 1.8
5/6 Nx+Los	16.6 ± 1.6	63 ± 2.0
5/6 Nx+MLN	15.4 ± 2.3	70 ± 1.9
5/6 Nx+MLN+Los	17.6 ± 2.2	67 ± 3.1
5/6 Nx+Ang-(1-7)	21.1 ± 3.9 *	65 ± 2.5
5/6 Nx+Ang-(1-7)+Los	18.0 ± 2.8	62 ± 1.8

20-25 glomeruli were analyzed per mouse per group (for each parameter)

Relative mesangial area was quantified by Sirius red staining, which detects collagen type IV fibers in the mesangium of the glomerulus. Values are reported as the percentage of total glomerular area that consists of mesangium.

Data are means ± standard errors

Data compared using one-way ANOVA followed by post-hoc Tukey's test

* $P < 0.05$ vs. Sham

[a] All groups were n=8 except for 5/6 Nx+MLN+Los. (n=7)

4.5: Pharmacological inhibition of ACE2 increases albuminuria in 5/6 Nx mice

The presence of albumin in the urine is termed albuminuria, and is considered a marker for the progression of kidney injury (Levey, Coresh et al. 2003). To evaluate the progression of kidney injury in each experimental group of mice, the urinary albumin excretion was measured and corrected for creatinine excretion.

At four weeks post 5/6 Nx, urinary albumin excretion was significantly increased in 5/6 Nx mice, compared to Sham mice (**Figure 4**). Treatment of 5/6 Nx mice with losartan tended to decrease urinary albumin excretion values, compared to 5/6 Nx mice. In 5/6 Nx mice, treatment with MLN further increased urinary albumin excretion values approximately three-fold, compared to vehicle-treated 5/6 Nx mice ($P < 0.001$ vs. 5/6 Nx). Interestingly, losartan treatment completely reversed the increase in urinary albumin excretion in 5/6 Nx mice treated with MLN. Administration of Ang-(1-7) to 5/6 Nx mice did not did not significantly affect urinary albumin excretion values

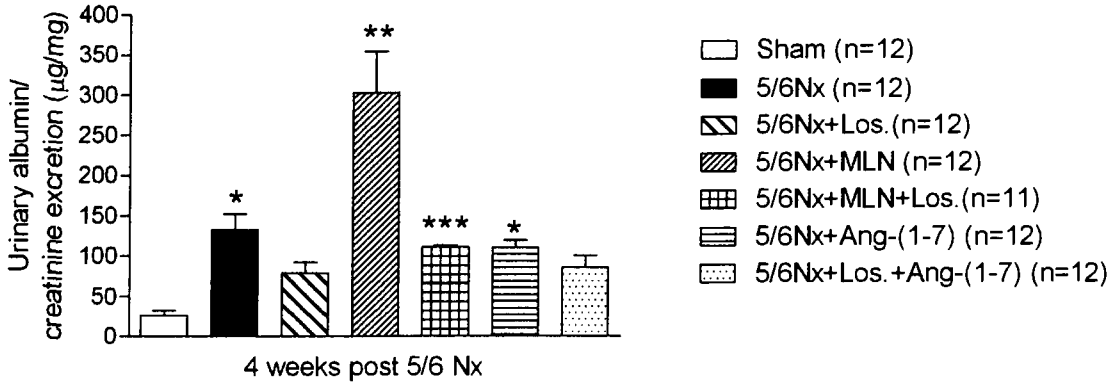

Figure 4. ACE2 inhibition increases albuminuria in 5/6 Nx mice.

Urinary albumin levels were measured on spot urine collections by ELISA and then corrected for creatinine excretion. Values are means ± S.E.M. Statistical comparisons were made using one-way ANOVA followed by Tukey's post-hoc test. * $P < 0.05$ vs. Sham, ** $P < 0.001$ vs. 5/6 Nx, and vs. Sham, *** $P < 0.001$ vs. 5/6 Nx+MLN, and vs. Sham.

4.6: Pharmacological inhibition of ACE2 in Sham mice

Based on the albuminuria data obtained from 5/6 Nx mice treated with MLN, it was important to determine if treatment of normal mice with MLN causes any adverse effects on blood pressure and measures of kidney function or albuminuria. Normal male FVB mice underwent sham surgery and were then administered MLN over a four week period. Sham mice without MLN treatment were used as a control group. Systolic blood pressure measurements and urinary albumin excretion measurements were performed weekly. FITC-inulin clearance was also measured at four weeks post sham surgery.

As shown in **Figure 5A** and **5B**, treatment of Sham mice with MLN did not significantly affect blood pressure or FITC-inulin clearance values, compared to Sham mice. Similarly, there were no statistical differences in urinary albumin excretion between Sham mice with and without MLN treatment (**Figure 5C**).

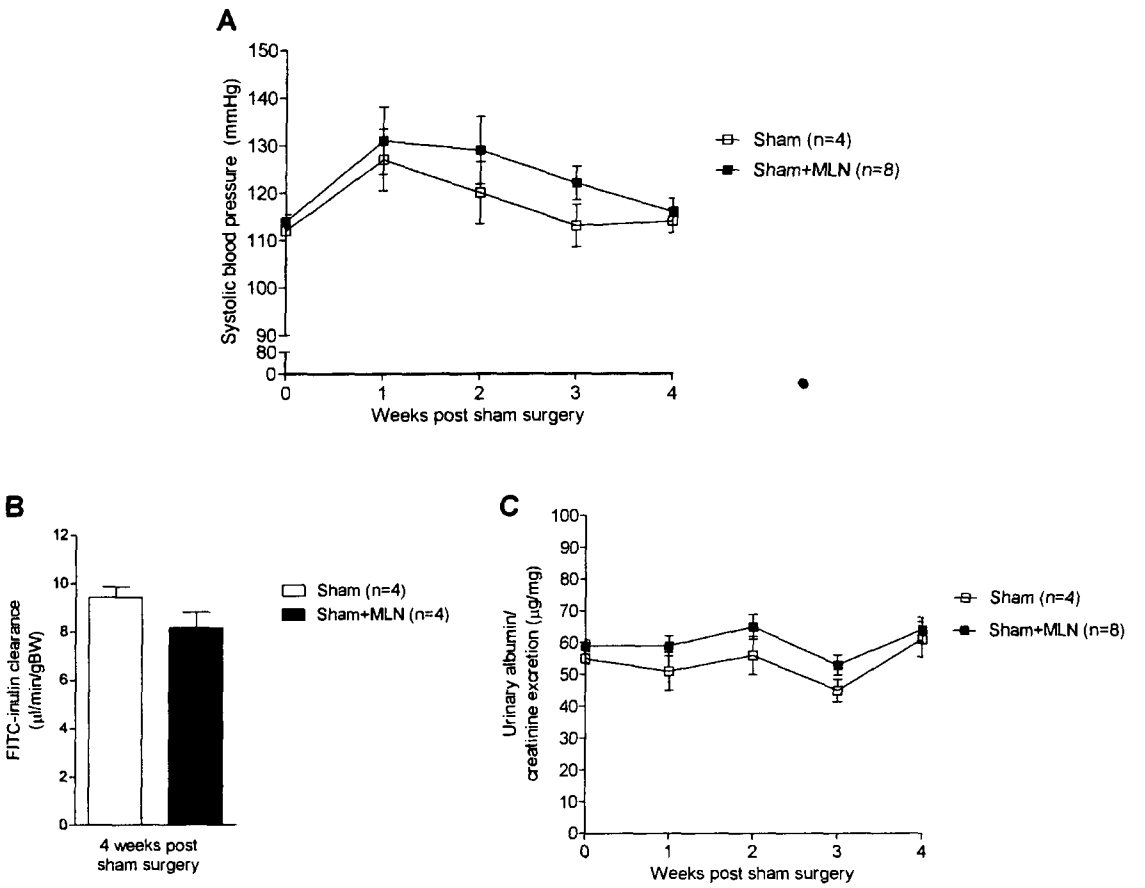

Figure 5. Blood pressure, FITC-inulin clearance, and urinary albumin excretion of Sham mice treated with MLN.

(**A**) Weekly systolic blood pressure measurements were performed by tail-cuff plethysmography. (**B**) Kidney function was assessed using the FITC-inulin clearance method. (**C**) Urinary albumin levels were measured on weekly spot urine collections by ELISA and then corrected for creatinine excretion. Values are means ± S.E.M. Statistical comparisons were made using Student's *t* test.

4.7: ACE2 is down-regulated in 5/6 Nx mice

As shown in **Figure 6A**, kidney cortex ACE2 protein expression is significantly decreased in 5/6 Nx mice with and without MLN treatment, compared to Sham mice. Treatment of 5/6 Nx mice with losartan or Ang-(1-7) did not significantly affect ACE2 protein expression. Similarly, as shown in **Figure 6B**, kidney cortex ACE2 activity tended to decrease in 5/6 Nx mice, compared to Sham mice. However, this decrease did not reach statistical significance. In 5/6 Nx mice, treatment with MLN significantly decreased kidney cortex ACE2 enzymatic activity, compared to Sham mice. In contrast, treatment of 5/6 Nx mice with losartan or Ang-(1-7) did not significantly affect ACE2 activity values.

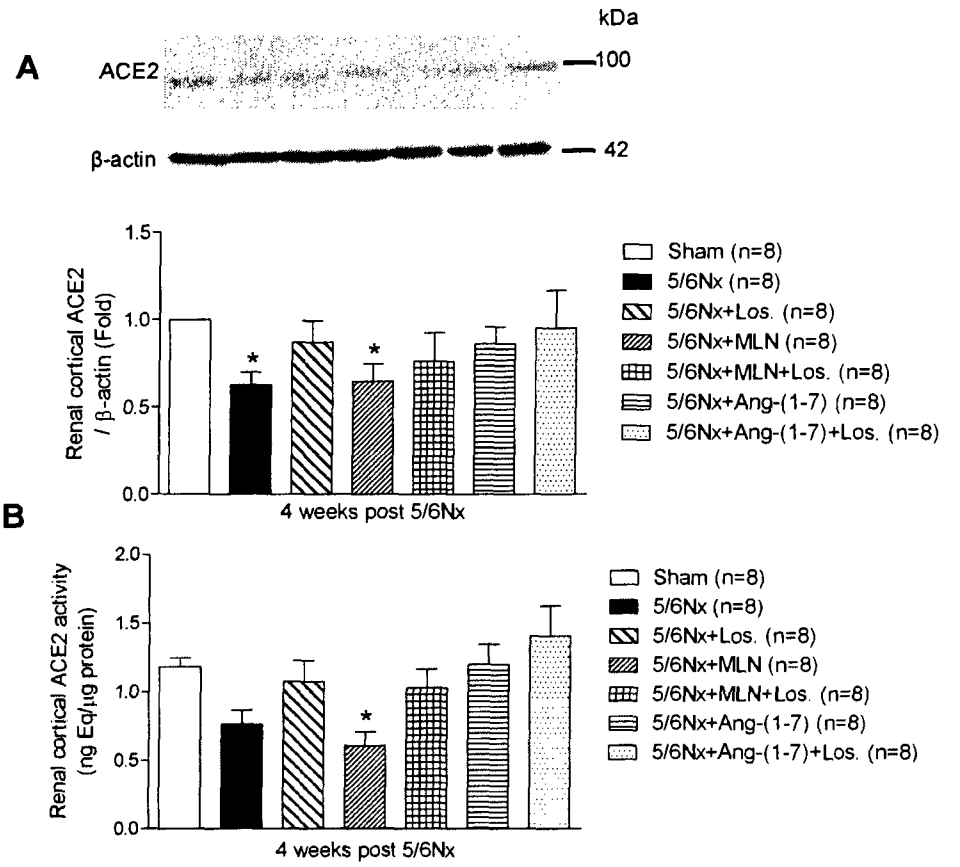

Figure 6. 5/6 Nx down-regulates kidney cortex ACE2 protein expression and activity.

(**A**) Kidney cortex ACE2 protein expression was measured by immunoblot using a specific ACE2 antibody (**Appendix: Table 5**). To control for protein loading, all membranes were stripped and reprobed with an antibody to β-actin. Displayed above the densitometric analysis is a representative immunoblot for ACE2 and the corresponding immunoblot for β-actin. Expression is presented as fold of Sham. (**B**) Kidney cortex ACE2 enzymatic activity was assayed at four weeks post 5/6 Nx using an ACE2-specific fluorogenic substrate. Values are means ± S.E.M. Statistical comparisons were made using one-way ANOVA followed by Tukey's post-hoc test. * $P < 0.05$ vs. Sham.

4.8: Kidney cortex expression of ACE in 5/6 Nx mice

As shown in **Figure 7**, kidney cortex ACE expression was not significantly altered in 5/6 Nx mice, compared to Sham mice. Similarly, no significant differences were observed between treatment groups of 5/6 Nx mice in terms of kidney cortex expression levels of ACE.

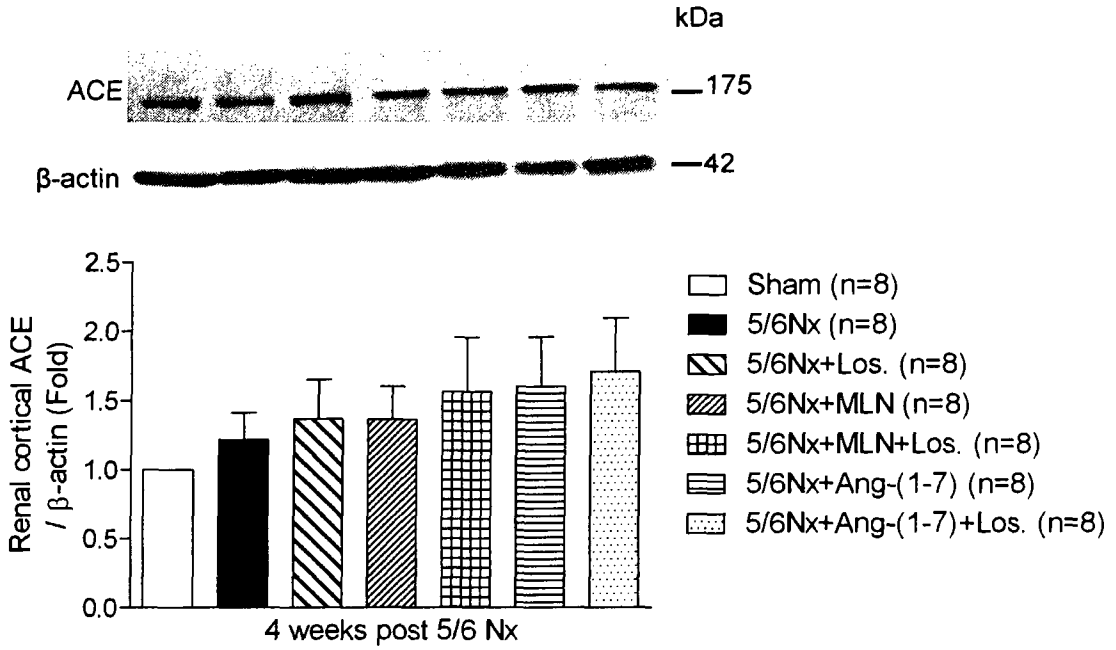

Figure 7. Kidney cortex ACE expression at four weeks post 5/6 Nx.

Kidney cortex ACE protein expression was measured by immunoblot using a specific ACE antibody (**Appendix: Table 5**). To control for protein loading, all membranes were stripped and reprobed with an antibody to β-actin. Displayed above the densitometric analysis is a representative immunoblot for ACE and the corresponding immunoblot for β-actin. Expression is presented as fold of Sham. Values are means ± S.E.M. Statistical comparisons were made using one-way ANOVA followed by Tukey's post-hoc test.

4.9: Kidney and plasma levels of Ang II and Ang-(1-7) in 5/6 Nx mice

Whole kidney and plasma measurements of Ang II were performed at four weeks post 5/6 Nx in order to further characterize the effects of ACE2 inhibition and Ang-(1-7) in 5/6 Nx mice. As shown in **Figure 8A**, 5/6 Nx is associated with a significant increase in kidney levels of Ang II, compared to Sham mice. Treatment of 5/6 Nx mice with either losartan or MLN did not significantly affect kidney levels of Ang II. In contrast, administration of Ang-(1-7) alone or Ang-(1-7) in combination with losartan tended to decrease kidney levels of Ang II, compared to 5/6 Nx mice. However, in both cases, the observed decrease in kidney Ang II levels did not reach statistical significance.

Plasma levels of Ang II were significantly increased in 5/6 Nx mice, compared to Sham mice (**Figure 8B**). Plasma levels of Ang II in 5/6 Nx mice were not affected by ACE2 inhibition or by administration of losartan. In contrast, administration of Ang-(1-7) to 5/6 Nx mice significantly decreased plasma Ang II levels, compared to 5/6 Nx mice. Similarly, treatment of 5/6 Nx mice with Ang-(1-7) in combination with losartan caused a modest but not significant decrease in plasma Ang II levels, compared to 5/6 Nx mice treated with either losartan alone or Ang-(1-7) alone.

No significant differences in whole kidney levels of Ang-(1-7) were observed between groups except that 5/6 Nx mice that were administered Ang-(1-7) exhibited a modest increase, compared to 5/6 Nx mice (**Figure 9A**). Plasma levels of Ang-(1-7) were not affected by 5/6 Nx (**Figure 9B**). Similarly, treatment of 5/6 Nx mice with MLN or losartan did not affect plasma levels of Ang-(1-7). In contrast, 5/6 Nx mice that were administered Ang-(1-7) exhibited an approximate 5-fold increase in plasma Ang-(1-7)

levels, compared to 5/6 Nx mice. This increase was significantly attenuated when Ang-(1-7) was co-infused with losartan in 5/6 Nx mice.

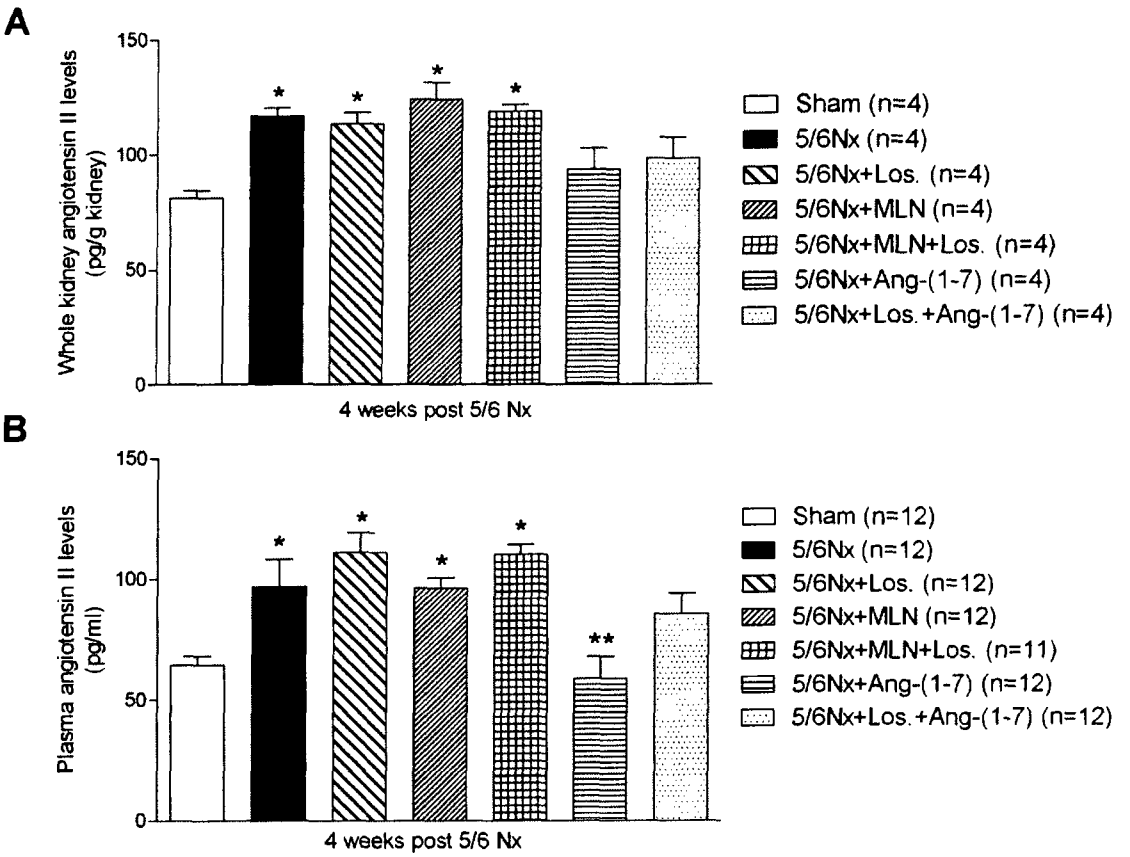

Figure 8. Whole kidney and plasma levels of Ang II at four weeks post 5/6 Nx.

Whole kidney (**A**) and plasma (**B**) levels of Ang II were measured by peptide radioimmunoassay utilizing an Ang II selective polyclonal antibody and ^{125}I-Ang II. Values are means ± S.E.M. Statistical comparisons were made using one-way ANOVA followed by Tukey's post-hoc test. * $P < 0.05$ vs. Sham, ** $P < 0.05$ vs. 5/6 Nx.

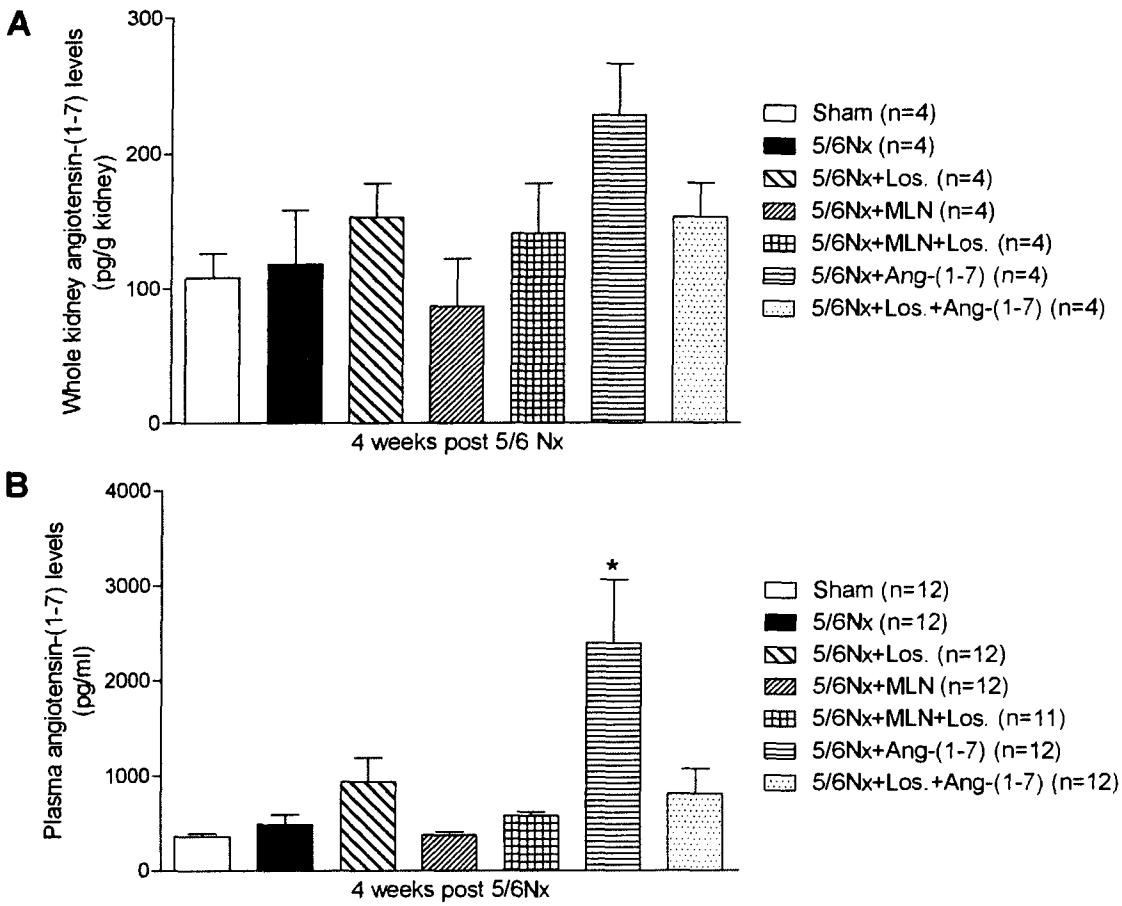

Figure 9. Whole kidney and plasma levels of Ang-(1-7) at four weeks post 5/6 Nx. Whole kidney (**A**) and plasma levels (**B**) of Ang-(1-7) were measured by peptide enzyme immunoassay utilizing an Ang-(1-7) selective polyclonal antibody. Values are means ± S.E.M. Statistical comparisons were made using one-way ANOVA followed by Tukey's post-hoc test. * $P < 0.05$ vs. Sham, 5/6 Nx, and remaining 5/6 Nx treatment groups.

4.10: Kidney cortex expression of phospho-p38 and phospho-ERK1/2 MAPK in 5/6 Nx mice

The effect of ACE2 inhibition and administration of Ang-(1-7) on AT_1 receptor signaling pathways was investigated in the context of non-diabetic kidney disease. In terms of p38 MAPK phosphorylation, no significant differences were observed between groups of mice (**Figure 10**). Similarly, no significant differences were observed between treatment groups of 5/6 Nx mice in terms of phosphorylation of ERK1/2 MAPK (**Figure 11**).

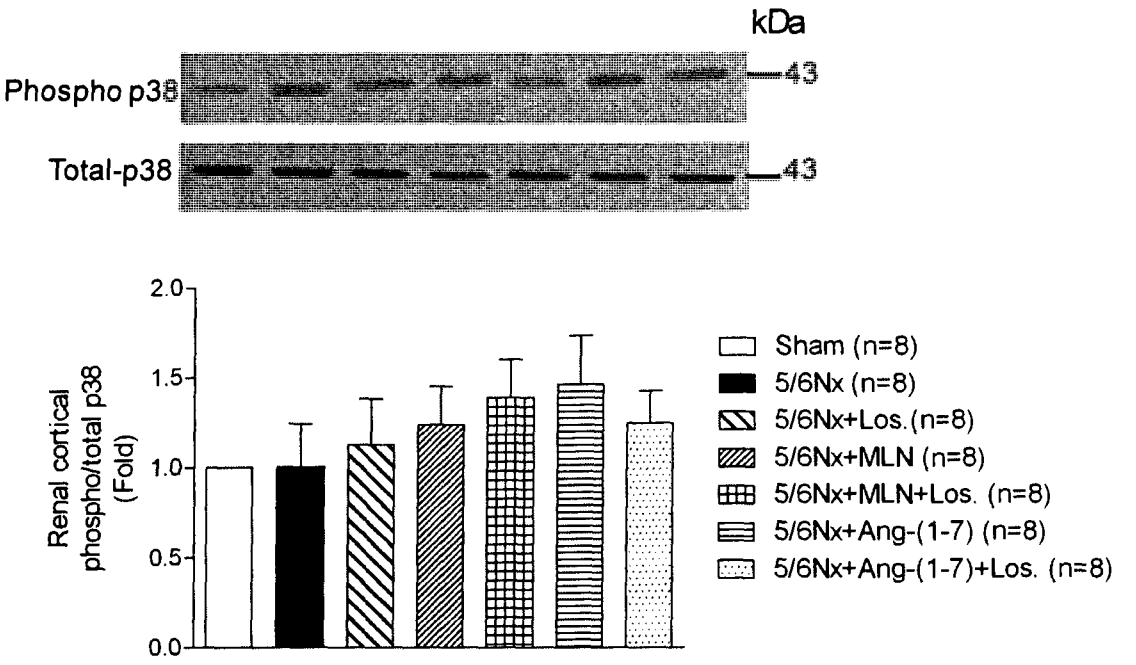

Figure 10. Kidney cortex expression of phospho p38 MAPK at four weeks post 5/6 Nx.

Kidney cortex phospho p38 MAPK protein expression was measured at four weeks post 5/6 Nx by immunoblot using a specific phospho p38 MAPK antibody (**Appendix: Table 5**). To control for protein loading, all membranes were stripped and reprobed with antibody that recognizes unphosphorylated and the phosphorylated p38 MAPK. Displayed above the densitometric analysis is a representative immunoblot for phospho p38 MAPK and the corresponding immunoblot for total p38 MAPK. Expression is presented as fold of Sham. Values are means ± S.E.M. Statistical comparisons were made using one-way ANOVA followed by Tukey's post-hoc test.

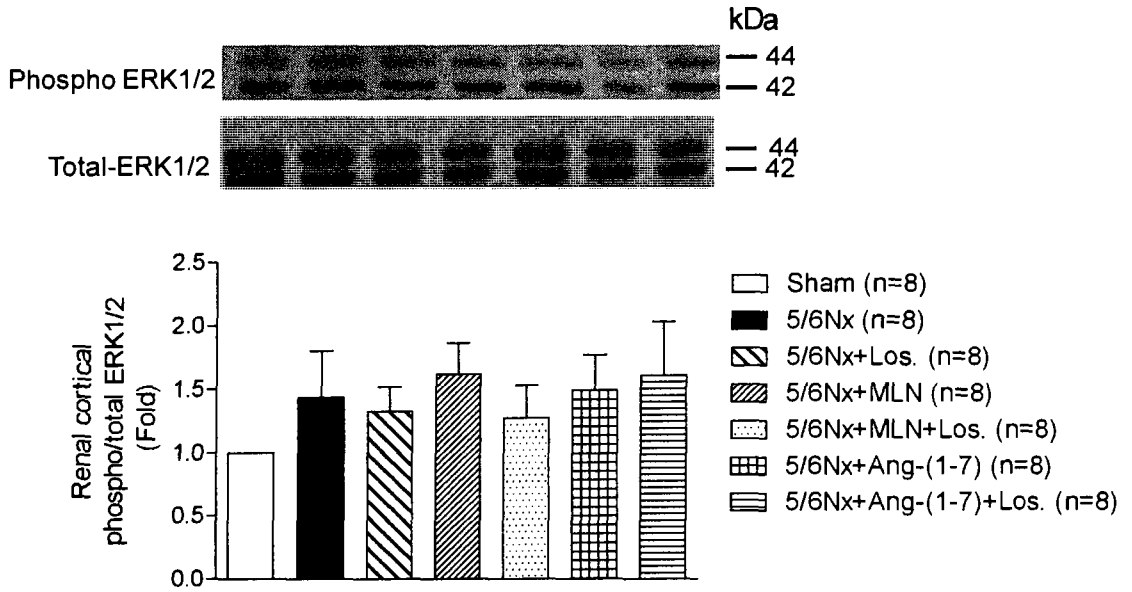

Figure 11. Kidney cortex expression of phospho ERK1/2 MAPK at four weeks post 5/6 Nx.

Kidney cortex phospho ERK1/2 MAPK protein expression was measured at four weeks post 5/6 Nx by immunoblot using a specific phospho ERK1/2 MAPK antibody (**Appendix: Table 5**). To control for protein loading, all membranes were stripped and reprobed with antibody that recognizes unphosphorylated and the phosphorylated ERK1/2 MAPK. Displayed above the densitometric analysis is a representative immunoblot for phospho ERK1/2 MAPK and the corresponding immunoblot for total ERK1/2 MAPK. Expression is presented as fold of Sham. Values are means ± S.E.M. Statistical comparisons were made using one-way ANOVA followed by Tukey's post-hoc test.

4.11: Kidney cortex expression of profibrotic markers in 5/6 Nx mice

To investigate whether ACE2 inhibition or administration of Ang-(1-7) affect the expression of certain profibrotic markers in 5/6 Nx mice, immunoblot analyses were performed at four weeks post 5/6 Nx for the following proteins: TGFβ1, VCAM-1, and α-SMA.

Kidney cortex TGFβ1 expression tended to increase in 5/6 Nx mice, compared to Sham mice (**Figure 12**). However, this increase did not reach statistical significance. Treatment of 5/6 Nx mice with either losartan, MLN or Ang-(1-7) did not alter kidney cortex expression of TGFβ1.

Similarly, kidney cortex expression of VCAM-1 in 5/6 Nx mice was comparable to that observed in Sham mice (**Figure 13**). Furthermore, VCAM-1 expression did not significantly differ between treatment groups of 5/6 Nx mice.

5/6 Nx was associated with a modest but not statistically significant increase in kidney cortex expression of α-SMA, compared to Sham mice (**Figure 14**). Treatment of 5/6 Nx mice with either MLN alone or MLN in combination with losartan did not significantly affect expression of α-SMA. Administration of Ang-(1-7) to 5/6 Nx mice significantly increased expression of α-SMA, compared to Sham mice but not to 5/6 Nx mice. This increase was attenuated when 5/6 Nx mice were treated with Ang-(1-7) in combination with losartan.

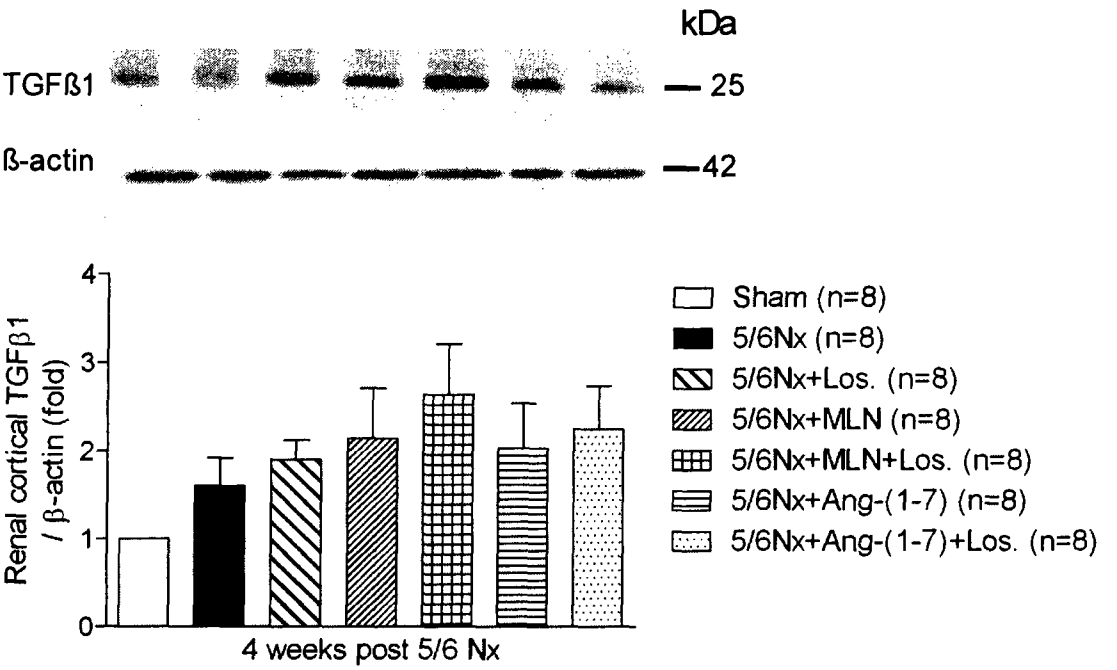

Figure 12. Kidney cortex expression of TGFβ1 at four weeks post 5/6 Nx.

Kidney cortex TGFβ1 protein expression was measured at four weeks post 5/6 Nx by immunoblot using a specific TGFβ1 antibody (**Appendix: Table 5**). To control for protein loading, all membranes were stripped and reprobed with an antibody to β-actin. Displayed above the densitometric analysis is a representative immunoblot for TGFβ1 and the corresponding immunoblot for β-actin. Expression is presented as fold of Sham. Values are means ± S.E.M. Statistical comparisons were made using one-way ANOVA followed by Tukey's post-hoc test.

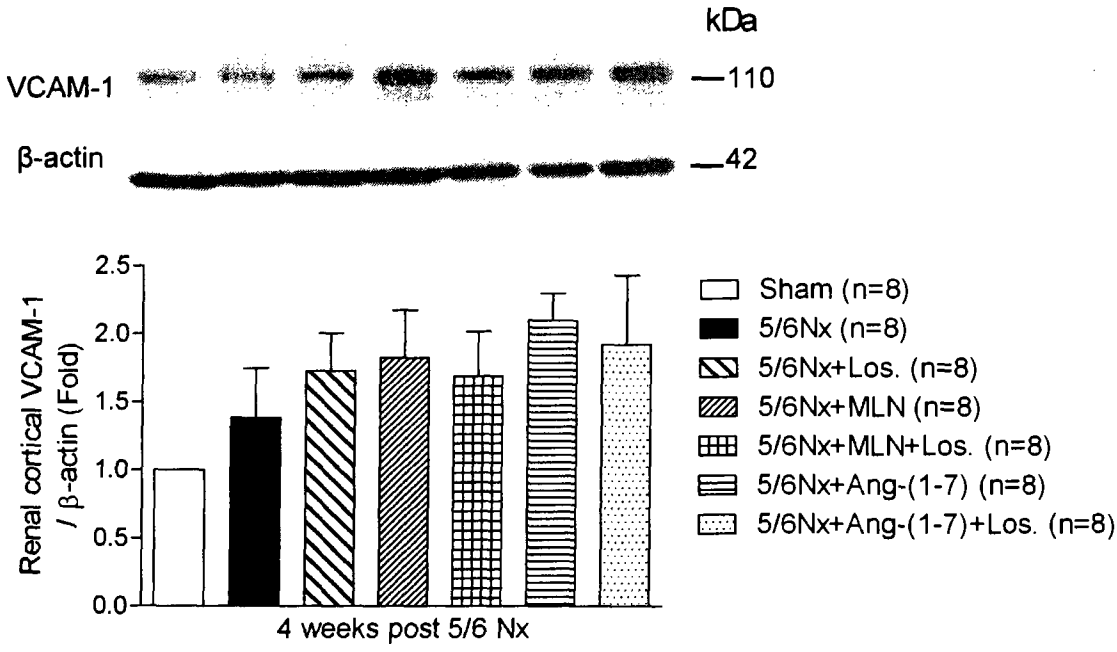

Figure 13. Kidney cortex expression of VCAM-1 at four weeks post 5/6 Nx.

Kidney cortex VCAM-1 protein expression was measured at four weeks post 5/6 Nx by immunoblot using a specific VCAM-1 antibody (**Appendix: Table 5**). To control for protein loading, all membranes were stripped and reprobed with an antibody to β-actin. Displayed above the densitometric analysis is a representative immunoblot for VCAM-1 and the corresponding immunoblot for β-actin. Expression is presented as fold of Sham. Values are means ± S.E.M. Statistical comparisons were made using one-way ANOVA followed by Tukey's post-hoc test.

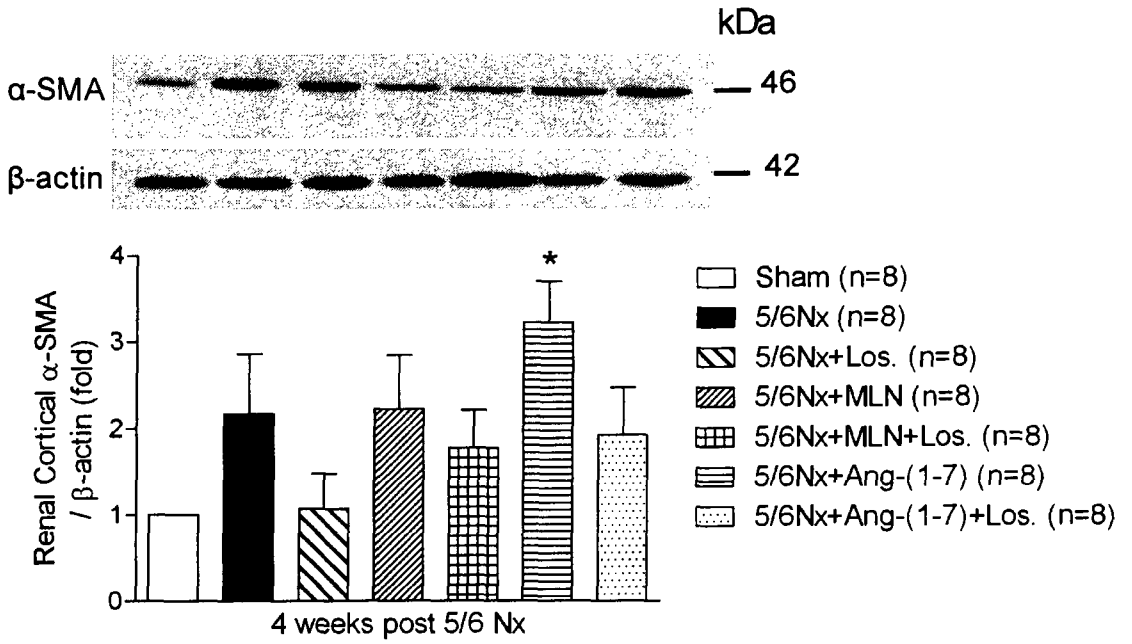

Figure 14. Kidney cortex expression of α-SMA at four weeks post 5/6 Nx.

Kidney cortex α-SMA protein expression was measured at four weeks post 5/6 Nx by immunoblot using a specific α-SMA antibody (**Appendix: Table 5**). To control for protein loading, all membranes were stripped and reprobed with an antibody to β-actin. Displayed above the densitometric analysis is a representative immunoblot for α-SMA and the corresponding immunoblot for β-actin. Expression is presented as fold of Sham. Values are means ± S.E.M. Statistical comparisons were made using one-way ANOVA followed by Tukey's post-hoc test. * $P < 0.05$ vs. Sham.

4.12: Long-term 5/6 Nx study

At four weeks, 5/6 Nx mice display limited kidney injury. Therefore, a twelve week 5/6 Nx study was conducted to investigate the long-term effects of 5/6 Nx on blood pressure, FITC-inulin clearance, and urinary albumin excretion. A small cohort of male FVB mice were subjected to 5/6 Nx and then euthanized at twelve weeks post 5/6 Nx. As a control group, normal male FVB underwent sham surgery and were also euthanized at twelve weeks following surgery.

As shown in **Figure 15A** and **15B**, at twelve weeks, both systolic blood pressure and urinary albumin excretion values were significantly increased in 5/6 Nx mice, compared to Sham mice. In contrast, FITC-inulin clearance values of 5/6 Nx mice were significantly decreased at twelve weeks, compared to Sham mice (**Figure 15C**).

The phenotype of 5/6 Nx mice at twelve weeks, was more severe than at four weeks. Blood pressure and urinary albumin excretion values were significantly increased in 5/6 Nx mice at twelve weeks compared to 5/6 Nx mice at four weeks (**Figure 16A** and **16B**). Furthermore, FITC-inulin clearance values were significantly decreased in 5/6 Nx mice at twelve weeks compared to 5/6 Nx mice at four weeks (**Figure 16C**). Therefore, we decided to pursue the effects of ACE2 inhibition and Ang-(1-7) at twelve weeks post 5/6 Nx. However, as we began our long-term 5/6 Nx study, we observed an extreme mortality rate (~90%) for 5/6 Nx mice. Despite many efforts to determine the cause of this high mortality rate, we were unable to complete the long-term 5/6 Nx study. Various measures were performed in an attempt to uncover the cause of death. For instance, different cautery apparati were tested, FVB/NJ mice from different suppliers were

ordered and underwent 5/6 Nx, and the pain medication for the 5/6 Nx mice was altered. A post-mortem analysis of the deceased 5/6 Nx mice revealed the likely cause of death to be sepsis. Nevertheless, we were unsuccessful in our attempt to determine the cause of bacterial infection in these mice. As a consequence, we were unable to complete the long-term 5/6 Nx study.

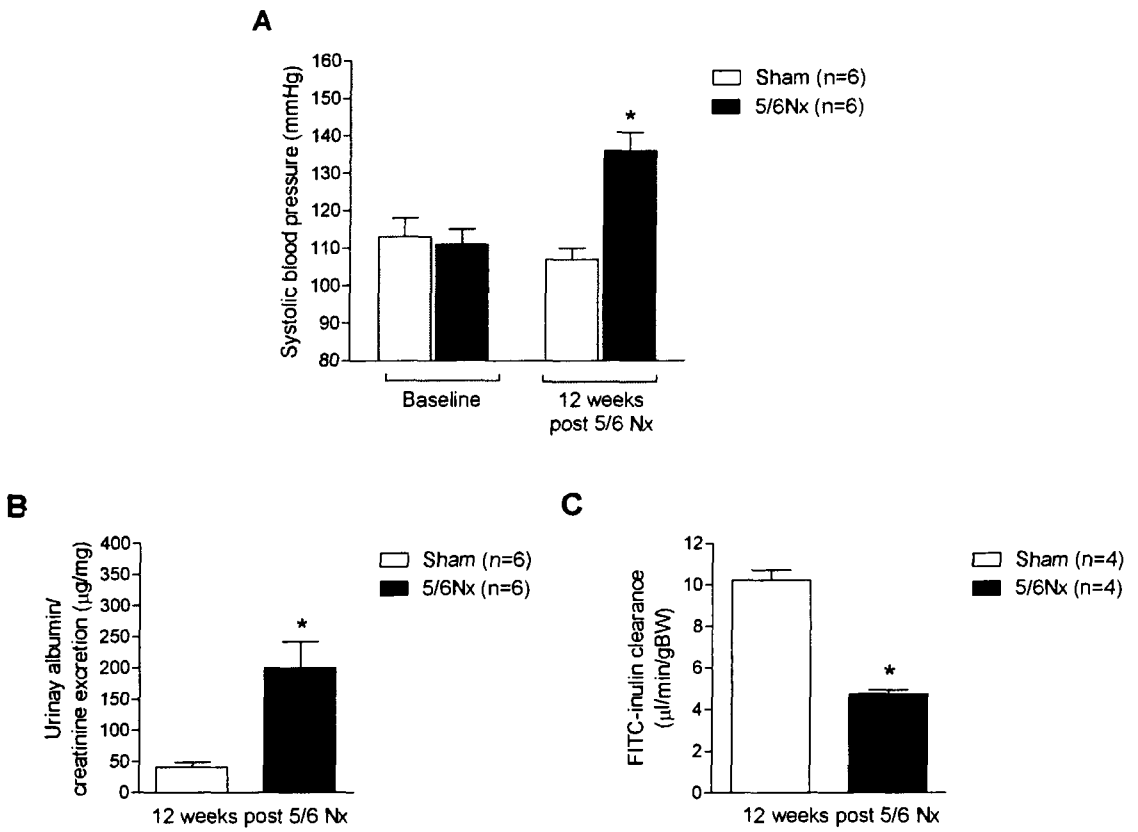

Figure 15. Blood pressure, urinary albumin excretion, and FITC-inulin clearance at twelve weeks post 5/6 Nx.

(**A**) Systolic blood pressure measurements were performed by tail-cuff plethysmography at baseline and twelve weeks post 5/6 Nx. (**B**) Urinary albumin levels were measured at twelve weeks on spot urine collections by ELISA and then corrected for creatinine excretion. (**C**) Kidney function was assessed using the FITC-inulin clearance method. Values are means ± S.E.M. Statistical comparisons were made using Student's *t* test. * $P < 0.05$ vs. Sham (at 12 weeks).

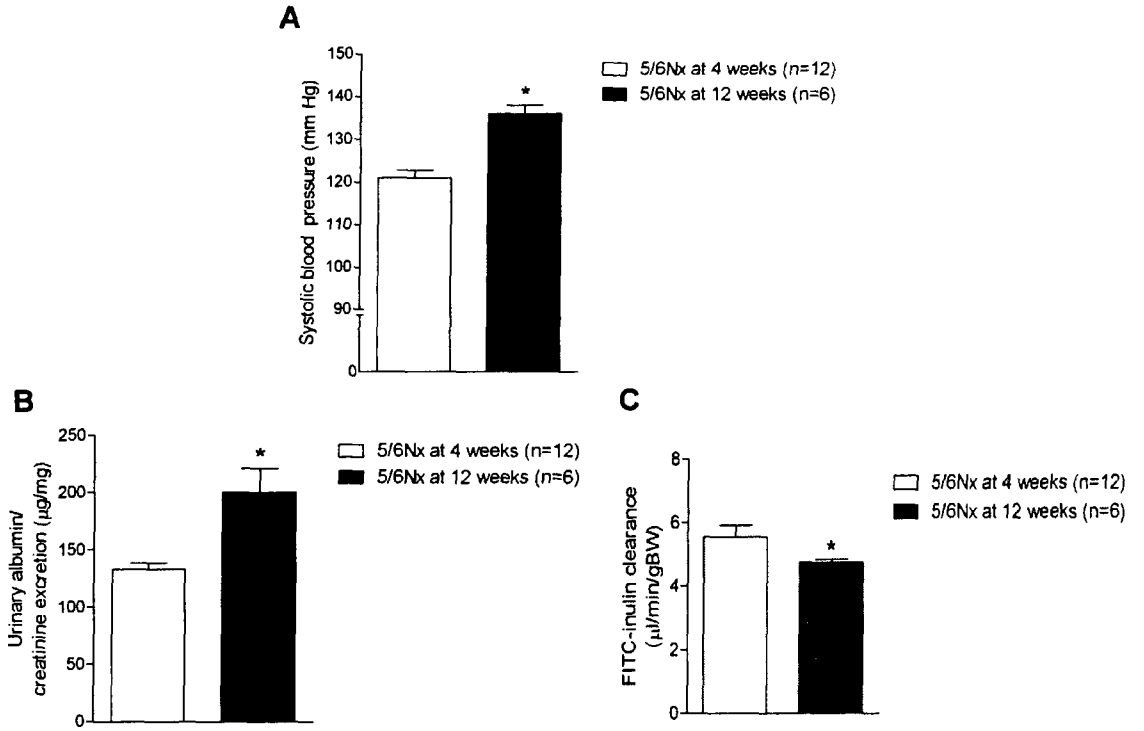

Figure 16. Comparison of blood pressure, urinary albumin excretion, and FITC-inulin clearance at four and twelve weeks post 5/6 Nx.

(**A**) Systolic blood pressure measurements were performed by tail-cuff plethysmography. (**B**) Kidney function was assessed using the FITC-inulin clearance method (**C**) Urinary albumin levels were measured on spot urine collections by ELISA and then corrected for creatinine excretion. (**C**) Kidney function was assessed using the FITC-inulin clearance method. Values are means ± S.E.M. Statistical comparisons were made using Student's *t* test. * $P < 0.05$ vs. 5/6 Nx at 4 weeks.

4.13: Generation of podocyte-specific ACE2 transgenic mice

In order to investigate the effects of ACE2 overexpression in the kidney, a transgenic mouse, which selectively expresses human ACE2 protein in the podocyte cells of the kidney, was created. This was achieved by first cloning an 8.3-kb fragment of the murine nephrin promoter (NP) immediately upstream of the human ACE2 open reading frame (hACE2 ORF) using *XhoI* restriction sites. Additionally, an N-terminal double-HA epitope tag (2XHA) was introduced to facilitate analysis of transgene expression *in vivo.* A restriction map of the NP-2XHA-hACE2 construct is displayed in **Figure 17**. Prior to microinjection, the transgene was sequenced in order to confirm the orientation of the transgene as well as the absence of mutations in the hACE2 ORF (data not shown).

Following microinjection of the NP-2XHA-hACE2 construct, several pups were born. All pups from the founder ACE2 transgenic mice were viable, fertile and display no physical abnormalities. Genomic DNA was isolated from each pup via tail snips. In order to determine if the transgene incorporated into the genomic DNA of the founder mice, specific primers which overlap the HA tag were utilized for genotypic analysis (**Figure 18A**). Out of 56 pups, 16 were identified as founder mice by PCR-based genotyping. Shown in **Figure 18B** is a representative genotypic analysis in which two out of the three candidate mice were identified as transgenic mice (lanes #2 and #3) based on the expected size of the PCR amplicon at 142 base pairs (Bp). Lane #1 represents a wild-type mouse since there is no band present at 142 Bp.

Subsequent characterization of the ACE2 transgenic mice was performed by Dr. Rosangela Milagres, a previous postdoctoral fellow in our laboratory.

Immunofluoresence data (not shown) from Dr. Milagres indicates that human ACE2 protein colocalizes with the podocyte marker synaptopodin in glomeruli from ACE2 transgenic mice.

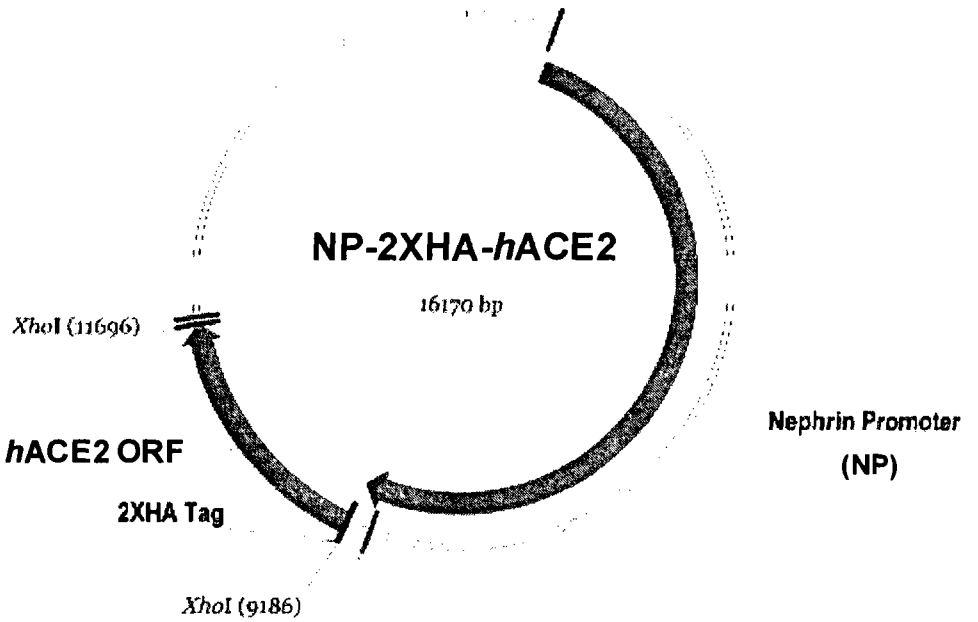

Figure 17. Restriction map of the NP-2XHA-hACE2 construct.

The human ACE2 open reading frame (hACE2 ORF) and a double hemagglutinin (2XHA) epitope tag were cloned upstream of an 8.3-kb fragment of the murine nephrin promoter (NP) using *Xho*I restriction sites. The resulting construct (NP-2XHA-hACE2) was used to generate ACE2 transgenic mice that selectively overexpress human ACE2 protein in the glomerular podocyte.

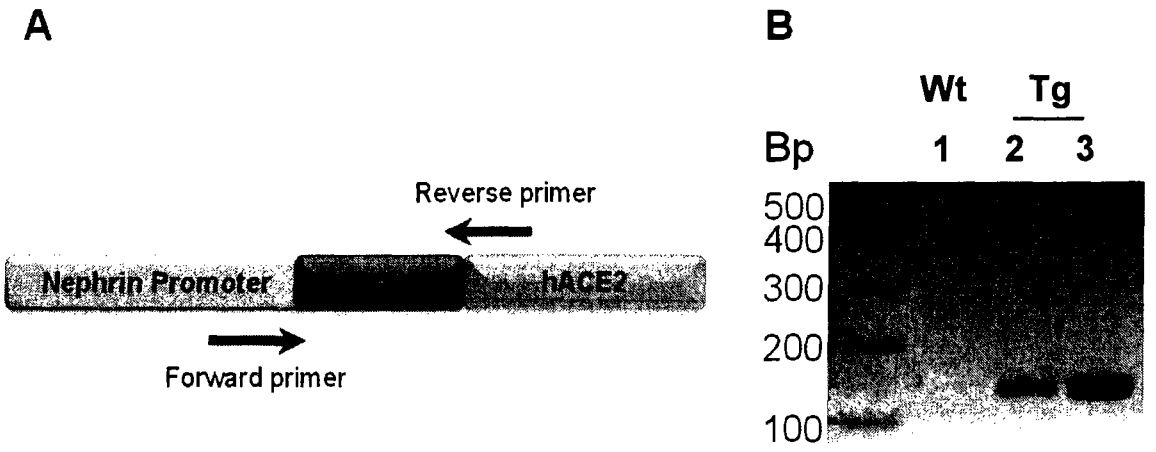

Figure 18. NP-2XHA-hACE2 construct and genotypic analysis.

(**A**) Schematic diagram of the NP-2XHA-hACE2 highlighting the fact that specific primers, which overlap the HA tag, were utilized in order to perform the genotypic analysis. (**B**) Genomic DNA was isolated from tail snips of resulting pups and PCR was performed in order to identify founders carrying the transgene of interest. PCR products were run on a 2.0% agarose gel. The expected size of the PCR amplicon is 142 base pairs (Bp). Shown is a representative picture of a gel with 3 candidate mice. Two out of the three mice express the transgene of interest (lanes #2 and #3). Therefore, these mice are considered as transgenic (Brinkkoetter, Holtgrefe et al.). Lane #1 does not have a band at 142 Bp and therefore, this mouse is considered wild-type (Wt).

4.14: Transfected COS-7 cells express functional recombinant ACE2 protein

In order to determine if the transgene of interest can yield functional recombinant human ACE2 protein, COS-7 cells were transfected with a vector (2XHA-hACE2) encoding the human ACE2 gene (hACE2) and a double HA tag. As a control, separate COS-7 cells were transfected with the empty PCDNA3 vector. 48 hours after transfection, protein lysates from untransfected COS-7 cells and COS-7 cells transfected with either vector alone, or 2XHA-hACE2 were isolated and resolved by SDS-PAGE. Human ACE2 protein expression was determined by immunoblot using a specific human ACE2 antibody (**Appendix: Table 5**). Protein lysates from untransfected COS-7 cells and COS-7 cells transfected with either the empty PCDNA3 vector, or 2XHA-hACE2 were isolated for the measurement of ACE2 enzymatic activity.

As shown in **Figure 19A**, a prominent band corresponding to human ACE2 (~100 kDa) was visualized in COS-7 cells transfected with the construct 2XHA-hACE2 (lane #3) but not in COS-7 cells transfected with the empty PCDNA3 vector (lane #2) or in untransfected COS-7 cells (lane #1). Similarly, after stripping and re-probing the immunoblot with a specific HA tag antibody (**Appendix: Table 5**), a band (~100 kDA) was only visualized in COS-7 cells transfected with the 2XHA-hACE2 construct (lane #3).

ACE2 activity could not be detected in untransfected COS-7 cells and COS-7 cells transfected with the empty PCDNA 3 vector (**Figure 19B**). In contrast, COS-7 cells transfected with the 2XHA-hACE2 construct displayed ACE2 enzymatic activity, which is completely inhibited following the addition of 1 μM MLN.

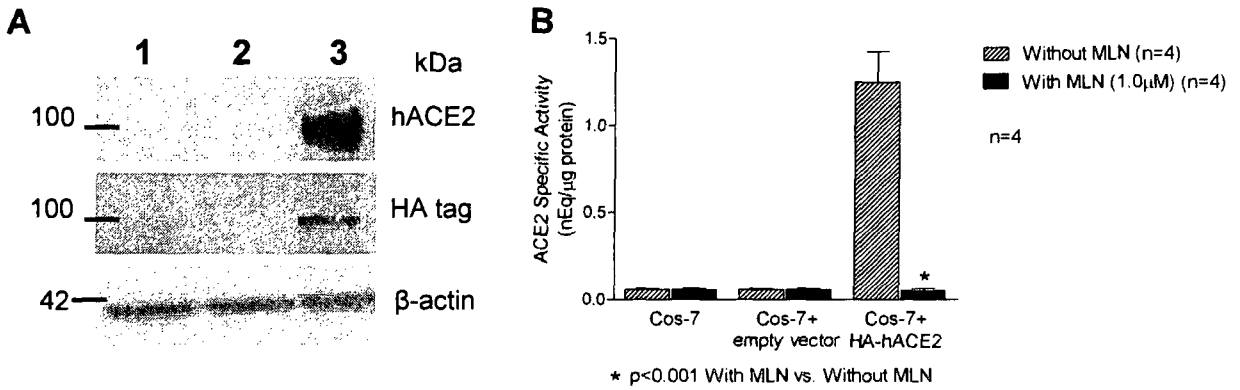

Figure 19. Transfected COS-7 cells express functional human ACE2 protein.

(**A**) Protein lysates from untransfected COS-7 cells (lane #1) and COS-7 cells transfected with either the empty PCDNA3 vector (lane #2), or 2XHA-hACE2 (lane #3) were resolved by SDS-PAGE. The immunoblot was probed with an anti-human ACE2 antibody (upper panel) and then stripped and reprobed with an anti-HA tag antibody (middle panel). The immunoblot was also probed with an antibody to β-actin antibody to verify equal protein loading (bottom panel). (**B**) Protein lysates from untransfected COS-7 cells and COS-7 cells transfected with either the empty PCDNA3 vector, or 2XHA-hACE2 were incubated with a specific ACE2 fluorogenic substrate in the presence or absence of 1.0 µM MLN in order to measure ACE2 enzymatic activity. Values are means ± S.E.M. Statistical comparisons were made using Student's *t* test. n= 4, * $P < 0.001$ vs. Cos-7+HA-ACE2 (without MLN).

5.0: Discussion

The primary goal of this study was to investigate the effects of ACE2 inhibition and the independent effects of Ang-(1-7) in a mouse model of CKD, namely the 5/6 nephrectomy mouse model of non-diabetic kidney disease. ACE2 is highly expressed in the kidney and mediates the conversion of Ang II to Ang-(1-7). At four weeks, induction of 5/6 Nx was associated with a modest but not significant increase in blood pressure, a 50% reduction in renal function, an increase in urinary albumin excretion, and a significant decrease in kidney cortex ACE2 protein expression. Pharmacological inhibition of ACE2 resulted in a further increase in urinary albumin excretion in 5/6 Nx mice. This effect was reversed by AT_1 receptor antagonism. Administration of Ang-(1-7) to 5/6 Nx mice increased relative mesangial area and kidney cortex expression of α-SMA. In contrast, Ang-(1-7) did not however, affect blood pressure or measures of renal function. In addition, we sought to develop ACE2 transgenic mice that selectively overexpress human ACE2 protein in the glomerular podocyte. The ACE2 transgenic mice were successful created and identified by genotypic analysis.

5.1: Use of a pharmacological inhibitor of ACE2 in 5/6 Nx mice

The effects of ACE2 inhibition were investigated in 5/6 Nx mice using a specific pharmacological inhibitor, MLN-4760 (MLN). We utilized this approach as opposed to the ACE2 knockout mouse for two distinct reasons. Firstly, since the inhibitor was administered to adult 5/6 Nx mice, the potential effects of ACE2 deficiency on kidney growth and development were avoided. Secondly, pharmacological inhibition of ACE2 resembles human kidney disease more closely in that it does not produce complete inhibition of ACE2 enzyme activity. The latter allows for the assessment of the relative importance of ACE2 in the progression of CKD. The specificity of MLN has previously been tested by Soler et al., who showed that MLN did not affect ACE activity in isolated glomeruli and renal cortex samples from C57BL/6 mice (Soler, Wysocki et al. 2007). Soler et al. also demonstrated that MLN completely inhibits the activity of recombinant mouse ACE2 protein (Soler, Wysocki et al. 2007).

5.2: Body weights, kidney weights, plasma analysis, and hematocrit measurements

Induction of 5/6 Nx was associated with significant compensatory kidney hypertrophy. This is evident by the remnant kidney weights of 5/6 Nx mice, which approached the weight of normal kidneys from Sham mice. In agreement with this finding, 5/6 Nx in rats is associated with significant remnant kidney hypertrophy (Sampaio-Maia, Serrao et al. 2005; Schafer, Lorenz et al. 1995). The loss of nephrons due to 5/6 Nx increases the workload of the remaining nephrons, leading to high intraglomerular filtration pressures and compensatory hypertrophy of the glomeruli and tubules (Levey, Coresh et al. 2003). Therefore, the remnant kidney hypertrophy that occurs following 5/6 Nx is an adaptive mechanism to maintain GFR. However, over time, this mechanism becomes maladaptive and leads to progressive kidney injury through various mechanisms. For example, increased intraglomerular pressure and hypertrophy cause detachment of the podocyte cells from the glomerular capillary wall and subsequent leakage of albumin into the urine (Griffin and Bidani 2006). Tubular hypertrophy leads to tubular atrophy and interstitial fibrosis as a result of increased production of reactive oxygen species, secretion of proinflammatory cytokines, and expression of extracellular matrix proteins (Levey, Coresh et al. 2003).

Plasma electrolytes were comparable between all groups of mice. However, urea levels were significantly increased in 5/6 Nx mice, compared to Sham. This finding was expected since urea and other metabolic waste products, which are normally excreted into the urine, are retained in the blood as CKD progresses (Gabizon, Goren et al. 1985).

Hematocrit values were significantly decreased in all 5/6 Nx treatment groups, compared to Sham mice. This data suggests that the 5/6 Nx mice were anemic, meaning

that they had a low red blood cell count, compared to healthy Sham mice. In humans, anemia is a common complication of progressive CKD (Griffin and Bidani 2006). 5/6 Nx may induce anemia as a result of diminished erythropoietin secretion. Erythropoietin is a peptide hormone that is involved in the control of red blood cell production by the bone marrow (Remuzzi, Ruggenenti et al. 2002).

5.3: Blood pressure responses in 5/6 Nx mice

Induction of 5/6 Nx was associated with a modest increase in systolic blood pressure at four weeks, compared to Sham mice. In CKD, hypertension contributes to progressive nephron loss by causing irreversible glomerular damage via increased intraglomerular pressure and glomerulosclerosis (Zoja, Abbate et al. 2006). The hypertensive response obtained in the 5/6 Nx model of CKD varies between genetic strains of mice (Kren and Hostetter 1999). For example, at four weeks post 5/6 Nx, Ma et al. reported that C57BL/6 mice display similar blood pressure values to control mice (approximately 100 mmHg) whereas 129/Sv mice exhibit elevated blood pressure values of approximately 160 mm Hg (Ma and Fogo 2003). The absence of significant hypertension in the vehicle-treated 5/6 Nx mice indicates that the genetic background of FVB mice may confer protection against the development of hypertension following renal mass reduction. In contrast, treatment of 5/6 Nx mice with losartan significantly reduced blood pressure. This finding was expected since losartan is commonly used for the treatment of hypertension in CKD (Weir 2009). Losartan decreases blood pressure by preventing Ang II from binding to AT_1 receptors.

Pharmacological inhibition of ACE2 in 5/6 Nx mice did not impact blood pressure values. This finding is in agreement with the phenotype of the ACE2 knockout mouse in which deletion of the ACE2 gene did not affect baseline blood pressures (Gurley, Allred et al. 2006). When 5/6 Nx mice were treated with a combination of MLN and losartan, blood pressure values did not decrease to same extent as when 5/6 Nx mice were treated with losartan alone. It is unclear why the losartan did not cause a significant decrease in blood pressure when combined with MLN, considering that treatment of 5/6 Nx mice with MLN alone did not affect blood pressure values.

Administration of Ang-(1-7) 5/6 Nx mice did not affect systolic blood pressure values. Consistent with this finding, in sodium-replete Wistar rats, Handa et al. demonstrated that Ang-(1-7) did not affect the decrease in renal blood flow induced by intrarenal bolus injection of Ang II (Handa, Ferrario et al. 1996). Although our data do not support a role for Ang-(1-7) in regulating blood pressure responses, Ang-(1-7) may regulate certain hemodynamic events in the renal vasculature. For instance, Ren et al. showed that Ang-(1-7) causes afferent arteriolar dilatation, mediated by production of NO (Ren, Garvin et al. 2002). The precise role of Ang-(1-7) in regulating blood pressure and renal hemodynamics is difficult to ascertain because renal blood flow is regulated by numerous vasoconstrictor and vasodilator influences. Therefore, it is possible that the renal hemodynamic effects of Ang-(1-7) may be masked *in vivo* (Navar, Inscho et al. 1996).

Combination therapy with losartan and Ang-(1-7) significantly decreased blood pressure values, compared to 5/6 Nx mice treated with losartan alone. Since treatment of 5/6 Nx mice with Ang-(1-7) alone did not affect blood pressure values, the observed

decrease in blood pressure when losartan was combined with Ang-(1-7) is likely due to the effect of losartan in preventing the actions of Ang II.

5.4: Decreased FITC-inulin clearance in 5/6 Nx mice

GFR is the standard measure of renal function and can be used as an index to measure the progression of CKD (Griffin and Bidani 2006). The clearance of creatinine is commonly used to estimate GFR. However, this method has its limitations. Mice have high levels of noncreatinine chromagens in their blood, which make it hard to interpret the creatinine levels (Meyer et al. 1985). Qi et al. developed an alternative approach to measuring renal function in mice, which is based on the clearance kinetics of FITC-inulin (Qi and Breyer 2009).

Induction of 5/6 Nx was associated with a 50% reduction in renal function, compared to Sham mice. There were no significant differences in FITC-inulin clearance between treatment groups of 5/6 Nx mice. The observed decrease in FITC-inulin clearance in 5/6 Nx mice was relatively mild and suggests that a moderate level of kidney damage occurred in these mice. As previously mentioned, the clinical syndrome of CKD is divided in terms of severity in five stages, which are based on the level of GFR (Levey, Coresh et al. 2003). Accordingly, a 50% reduction of GFR in humans would be characterized as Stage 3 of CKD.

5.5: Kidney histological analyses

Histological analyses revealed a trend towards an increase in glomerular diameter in all 5/6 Nx treatment groups, compared to Sham. This effect was likely due to the increased glomerular capillary pressure that occurs following renal mass reduction (Remuzzi, Ruggenenti et al. 2002). Following 5/6 Nx, the remaining glomeruli of the remnant kidney hypertrophy in order to compensate for reduced nephron number and to preserve renal function (Schlondorff 2008). Increased glomerular capillary pressure in turn causes mesangial cell hypertrophy and matrix expansion.

Mesangial area was quantified using sections of remnant kidney stained with Sirius red, which stains collagen type IV. Induction of 5/6 Nx caused a trend towards an increase in relative mesangial area, compared to Sham mice. However, no significant differences between the 5/6 Nx treatment groups were observed. The lack of significant mesangial expansion in 5/6 Nx mice is probably reflective of the early time point at which the mice were euthanized. In contrast, treatment of 5/6 Nx with Ang-(1-7) significantly increased relative mesangial area, compared with Sham mice. This data suggest that Ang-(1-7) may stimulate expression of profibrotic factors in mesangial cells. Consistent with this finding, Zimpelmann and Burns showed that Ang-(1-7) significantly increased production of TGFβ1, fibronectin, and collagen type IV in cultured human mesangial cells (Zimpelmann and Burns 2009).

Following 5/6 Nx in rats, the remnant kidney typically advances through three separate histological phases: phase 1, kidney hypertrophy appears at 2-4 weeks following 5/6 Nx; phase 2, detectable changes in the residual renal mass occur up to 10 weeks; and

phase 3, glomerulosclerosis and interstitial fibrosis become apparent at ten weeks (Zoja, Abbate et al. 2006). The absence of major pathological changes in 5/6 Nx mice suggests that at four weeks, 5/6 Nx mice displayed a relatively mild form of CKD.

5.6: ACE2 is down-regulated in 5/6 Nx mice

At four weeks, kidney cortex ACE2 expression was significantly decreased in 5/6 Nx mice, compared to Sham mice. This is in agreement with human and mouse studies whereby kidney expression of ACE2 is down-regulated in diabetic kidney disease (Mizuiri, Hemmi et al. 2008; Reich, Oudit et al. 2008; Tikellis, Johnston et al. 2003; Ye, Wysocki et al. 2004; Ye, Wysocki et al. 2006). Similarly, in a study performed in unilaterally nephrectomized rats loaded with bovine plasma albumin as a model of proteinuric renal injury, kidney ACE2 protein expression was decreased (Takase, Marumo et al. 2005), an effect associated with tubuloinsterstitial injury. In our study, it is not known whether the observed decrease in kidney ACE2 expression occurred at the level of the proximal tubule and/or the glomerulus. Further studies using isolated glomeruli and renal tubules would permit a more accurate assessment of the renal expression pattern of ACE2 in 5/6 Nx mice. Treatment of 5/6 Nx mice with MLN mice did not alter ACE2 protein expression. This finding is expected since MLN functions as an inhibitor of ACE2 enzymatic activity. Likewise, administration of Ang-(1-7) to 5/6 Nx did not alter ACE2 protein expression. Since ACE2 catalyzes the formation of Ang-(1-7), one might expect that infusion of Ang-(1-7) would cause a negative feedback mechanism thereby attenuating kidney ACE2 protein expression. However, due to the

short half-time of Ang-(1-7), it is unlikely that this regulatory event would occur (Trask and Ferrario 2007).

The kidney cortex ACE2 enzymatic activity data is consistent with the ACE2 immunoblot data. Accordingly, at four weeks post 5/6 Nx, ACE2 activity levels tended to decrease in 5/6 Nx mice, compared to Sham mice. Treatment of 5/6 Nx mice with MLN caused a further reduction in ACE2 activity that was significant compared to Sham mice. Due to the experimental design of the fluorogenic assay used to measure ACE2 activity levels, it is possible that the MLN compound may dislodge from the ACE2 protein during the homogenization process of the kidney samples. This in turn, could lead to inaccurate measurements of ACE2 enzymatic activity in 5/6 Nx mice treated with MLN. Lastly, treatment of 5/6 Nx mice with losartan caused a modest but not significant increase in both kidney cortex ACE2 protein expression and ACE2 activity, compared to Sham mice.

5.7: ACE2 inhibition increases albuminuria in 5/6 Nx mice

5/6 Nx was associated with a significant increase in urinary albumin excretion, compared to Sham mice. In 5/6 Nx mice with MLN treatment, urinary albumin excretion was increased by three-fold, compared to vehicle-treated 5/6 Nx mice. This data is consistent with the reported effects of ACE2 inhibition in diabetic mice. Treatment of STZ-induced diabetic mice with MLN, for a period of four weeks, significantly increased urinary albumin excretion, compared to control mice (Soler, Wysocki et al. 2007). Similarly, chronic inhibition of ACE2 in db/db diabetic mice resulted in a three-fold

increase in urinary albumin excretion that was independent of blood pressure changes when compared to vehicle-treated db/db mice (Ye, Wysocki et al. 2006). Our data suggest that ACE2 is renoprotective in non-diabetic CKD by limiting urinary albumin excretion.

To determine if this response is mediated by Ang II, the effects of the AT_1 receptor antagonist losartan were studied in 5/6 Nx mice, with or without ACE2 inhibition. Losartan-treated 5/6 Nx mice displayed a trend towards a decrease in urinary albumin excretion that was not significant, compared to vehicle-treated 5/6 Nx mice. Interestingly, combination therapy of losartan and MLN completely reversed the increase in urinary albumin excretion that was observed upon inhibition of ACE2 in 5/6 Nx mice. In agreement with these data, in db/db diabetic mice, treatment with MLN increased albuminuria, an effect that was reversed by AT_1 receptor antagonism (Ye, Wysocki et al. 2006). Therefore, these data suggest that in non-diabetic kidney disease, ACE2 inhibition increases urinary albumin excretion via an AT_1 receptor-dependent mechanism.

5.8: ACE2 inhibition in Sham mice

Wild-type FVB/NJ mice underwent sham surgery and were treated with MLN for a period of four weeks to determine if pharmacological inhibition of ACE2 affects blood pressure and measures of renal function in healthy mice. In comparison to vehicle-treated Sham mice, MLN treatment did not impact blood pressure, FITC-inulin clearance, or urinary albumin excretion values. Similarly, Tikellis et al. reported that treatment of wild-type C57BL/6 with MLN at a dose of 10 mg/kg/day did not affect systolic blood

pressure or creatinine clearance (Tikellis, Bialkowski et al. 2008). However, urinary albumin excretion values were significantly lower in wild-type C57BL/6 mice treated with MLN, compared to control mice in their study. Experimental design differences may contribute to the discrepancy in urinary albumin excretion values following treatment with MLN. For instance, the dose of MLN in our study was eight times higher than that used in the Tikellis et al. study. Moreover, the MLN in our study was administered by subcutaneous injection rather than in the drinking water as in the Tikellis et al. study. More importantly, it is conceivable that genetic differences between mouse strains may account at least in part, for this discrepancy.

5.9: Kidney cortex expression of ACE in 5/6 Nx mice

Kidney cortex expression of ACE was similar between all groups of mice. In contrast, Soler et al. reported a dichotomy between glomerular ACE and tubular ACE expression in the context of diabetic kidney disease (Soler, Wysocki et al. 2007). In STZ-induced diabetic mice, glomerular and vascular expression of ACE was increased, however, in the kidney cortex, which consists predominantly of renal tubules, ACE was decreased both at the level of mRNA and enzymatic activity, compared to non-diabetic control mice.

ACE and ACE2 work as counter-regulatory enzymes in order to regulate the level of angiotensin peptides (Vickers, Hales et al. 2002). Therefore, a combination of high ACE and low ACE2 in the glomerulus, favors the formation of Ang II, which could promote the progression of renal injury. In db/db diabetic mice, Ye et al. reported reduced expression of ACE in the kidney cortex, whereas ACE2 protein expression in the

kidney cortex was increased (Ye, Wysocki et al. 2004). The significance of a reduction in ACE coupled with an increase in ACE2 is unclear, however, it is plausible that such combination would attenuate Ang II formation and could potentially exert a renoprotective effect against the progression of diabetic CKD. In the context of non-diabetic CKD, future experiments using isolated renal tubules and glomeruli from 5/6 Nx mice may provide further information concerning the role of ACE in relation to ACE2.

5.10: Kidney and plasma levels of Ang II and Ang-(1-7) in 5/6 Nx mice

Measurements of Ang II and Ang-(1-7) were performed in whole kidney and plasma samples to further characterize the effects of ACE2 inhibition and Ang-(1-7) in 5/6 Nx mice. Induction of 5/6 Nx resulted in a significant increase in both whole kidney and plasma levels of Ang II, compared to Sham. Increases in intrarenal RAS components, particularly Ang II, have been demonstrated in progressive CKD in both rats and humans (Graciano, Cavaglieri Rde et al. 2004; Sadhu, Domingue et al. 1989). In 5/6 Nx mice, treatment with MLN did not cause a further increase in either whole kidney or plasma levels of Ang II. These data are in agreement with studies performed in both STZ-induced diabetic mice and ACE2 knockout mice, whereby whole kidney and plasma levels of Ang II were not significantly different than control mice (Soler, Wysocki et al. 2007; Wong, Oudit et al. 2007).

In contrast, Ang-(1-7) significantly decreased plasma levels of Ang II in 5/6 Nx mice. Similarly, whole kidney levels of Ang II tended to decrease in 5/6 Nx mice treated with Ang-(1-7), compared to vehicle-treated 5/6 Nx mice. ACE converts Ang I to Ang II but also Ang-(1-9) to Ang-(1-7) (Agata, Ura et al. 2006). Li et al. have reported that

Ang-(1-7) inhibits purified recombinant ACE enzymatic activity (Li, Chappell et al. 1997). Therefore, administration of Ang-(1-7) to 5/6 Nx mice may inhibit renal and plasma ACE enzymatic activity in order to limit further production of Ang-(1-7). In doing so, this would also limit the formation of Ang II.

Whole kidney and plasma levels of Ang-(1-7) were not significantly different between vehicle-treated 5/6 Nx mice and Sham mice. However, treatment of 5/6 Nx mice with losartan tended to increase plasma levels of Ang-(1-7). In both rats and humans, chronic treatment with AT_1 receptor blockers increases plasma levels of Ang-(1-7) (5- to 25-fold) (Campbell, Lawrence et al. 1991; Kohara, Brosnihan et al. 1991; Kohara, Brosnihan et al. 1993; Luque, Martin et al. 1996). Antagonism of AT_1 receptors increases Ang-(1-7) levels, presumably by increasing plasma levels of Ang II, which can be converted to Ang-(1-7) by ACE2. Treatment of 5/6 Nx mice with MLN did not alter renal and plasma levels of Ang-(1-7).

Plasma levels of Ang-(1-7) were approximately seven-fold higher in Ang-(1-7)-infused 5/6 Nx mice, compared to vehicle-treated 5/6 Nx mice. This data served as positive control and validated the enzyme immunoassay that was used to measure whole kidney and plasma levels of Ang-(1-7). Moreover, the effect of increased plasma levels of Ang-(1-7) levels in 5/6 Nx mice treated with Ang-(1-7), was reversed by combination therapy with Ang-(1-7) and losartan. Since administration of either Ang-(1-7) alone or losartan alone are known to increase plasma levels of Ang-(1-7), the combination of both drugs may have triggered a compensatory response aimed at decreasing circulation levels of Ang-(1-7). In this regard, ACE has been shown to metabolize Ang-(1-7) to angiotensin-(1-5) in the systemic vasculature (Chappell, Pirro et al. 1998; Deddish,

Marcic et al. 1998). Therefore, it is possible that the combination of losartan and Ang-(1-7) may have caused upregulation of ACE in the systemic vasculature, thus leading to increased metabolism of Ang-(1-7).

The data from the measurements of renal levels of Ang II and Ang-(1-7) are difficult to interpret since whole kidney lysates were used for each these measurements. In order to precisely examine intrarenal levels of angiotensin peptides, measurements of Ang II and Ang-(1-7) would have to be performed using isolated renal tubules and glomeruli.

5.11: Kidney cortex expression of phospho-p38 and phospho-ERK1/2 MAPK in 5/6 Nx mice

Chronic activation of the AT_1 receptor is a central event in the progression of CKD (Schlondorff 2008). The binding of Ang II to AT_1 receptors in the kidney results in activation of MAPK signaling cascades. Phosphorylation of p38 and ERK1/2 MAPKs were not significantly altered in 5/6 Nx mice, compared to Sham mice. No significant differences were observed between treatment groups of 5/6 Nx mice. Although ACE2 inhibition increased urinary albumin excretion in 5/6 Nx mice via an AT_1 receptor-dependent mechanism, we were unable to detect activation of downstream MAPK signaling pathways. In this regard, it is possible that under conditions of ACE2 inhibition, local activation of p38 or ERK1/2 signaling pathways within glomeruli may contribute towards increased urinary albumin excretion. For instance, studies by Hamaguchi et al. provided *in vivo* evidence that Ang II infusion led to activation of

glomerular ERK1/2 and JNK MAPKs, followed by an increase in arterial pressure (Hamaguchi, Kim et al. 1998).

5.12: Kidney cortex expression of profibrotic markers in 5/6 Nx mice

Renal fibrosis is a prominent feature of CKD that leads to an accumulation of extracellular matrix proteins and subsequent renal injury (Schlondorff 2008). Irrespective of the cause, CKD is characterized by scarring of the glomeruli (glomerulosclerosis) and tubulointerstitial fibrosis (Remuzzi, Ruggenenti et al. 2002). The development of fibrosis in non-diabetic kidney disease is typically associated with an increase in profibrotic and proinflammatory factors such as TFGβ1 and VCAM-1, respectively. Kidney cortex TGFβ1 expression was modestly increased in 5/6 Nx mice, compared to Sham mice. However, no significant differences were observed among treatment groups of 5/6 Nx mice. VCAM-1 is an immunoglobulin-like adhesion molecule expressed on activated endothelial cells VCAM-1 promotes monocyte adhesion (Khwaja, El Kossi et al. 2007). Accordingly, kidney cortex expression levels of VCAM-1 were comparable between all groups of mice. Increases in kidney cortex expression of TFGβ1 and VCAM-1 have been previously been reported at eight and twelve weeks post 5/6 Nx in rats (Taal, Zandi-Nejad et al. 2000). Kidney cortex expression of TFGβ1 and VCAM-1 expression did not significantly change in our model of CKD most likely because 5/6 Nx mice display a limited amount kidney injury at four weeks post 5/6 Nx.

De novo expression of α-SMA in myofibroblast cells is a key feature of CKD (Khwaja, El Kossi et al. 2007). The latter serves as a marker for epithelial-to-mesenchymal transition, which is a process that involves the transformation of renal

tubular cells from an epithelial to a mesenchymal phenotype (Remuzzi, Ruggenenti et al. 2002). In 5/6 Nx mice, there was a modest but not significant increase in kidney cortex expression of α-SMA, compared to Sham mice. Inhibition of ACE2 did not affect kidney cortex levels of α-SMA. In contrast, infusion of Ang-(1-7) in 5/6 Nx mice significantly increased expression of α-SMA, compared to Sham mice. This data argues against a renoprotective role for Ang-(1-7) in non-diabetic CKD. In this regard, Shao et al. showed that chronic infusion of Ang-(1-7) to STZ-diabetic male rats accelerates renal injury (Shao, He et al. 2008). Ang-(1-7) increased proteinuria as well as TGF-β1 mRNA and protein levels in the diabetic kidney, when compared to untreated diabetic rats.

5.13: Long-term 5/6 Nx study

The data from the four week 5/6 Nx study revealed limited kidney injury. However, by twelve weeks, the phenotype of the 5/6 Nx mouse was more severe than that observed at four weeks. Blood pressure and urinary albumin excretion values were significantly increased in 5/6 Nx mice at twelve weeks, compared to 5/6 Nx mice at four weeks. Renal function was also significantly decreased in 5/6 Nx mice at twelve weeks, compared to 5/6 Nx mice at four weeks. These data suggest that over time, 5/6 Nx in FVB mice leads to progressive renal injury. In agreement with these data, Ma et al. reported that blood pressure and urinary albumin excretion in 129/Sv mice were increased significantly after 5/6 Nx from four to twelve weeks (Ma and Fogo 2003).

Based on the data from the twelve week study, we sought to investigate the long-term effects of ACE2 inhibition and Ang-(1-7) in 5/6 Nx mice. At the start of the long-term 5/6 Nx study, we observed an extreme mortality rate (~90%) for 5/6 Nx mice. The

expected mortality rate of 5/6 Nx mice is approximately 10-20% (Kren and Hostetter 1999). Despite this setback, future studies focused on the long-term effects of ACE2 inhibition and Ang-(1-7) potentially could be completed by modifying the protocol of the 5/6 Nx surgical procedure. For example, 5/6 Nx can be achieved by removal of one kidney combined with infarction of two thirds of the remaining kidney rather than using cautery in order to reduce renal mass (Kren and Hostetter 1999). The advantage of the former method is that it does not involve significant blood loss or scarring of renal tissue. Moreover, the infarction method is relatively simple and less time-consuming that the two-step 5/6 Nx approach.

5.14: Transfected COS-7 cells express functional recombinant ACE2 protein

ACE2 transgenic mice were created in order to further characterize the physiological role of ACE2 in the kidney. These mice were generated by creating a specific ACE2 transgene that consisted of the nephrin promoter (NP), a double HA tag (2XHA), and the open reading frame of human ACE2 (hACE2 ORF). However, in order to determine if the ACE2 transgene could yield functional recombinant human ACE2 protein, transfection experiments were conducted using COS-7 cells.

In cells transfected with the 2XHA-hACE2 vector, immunoblot analysis revealed a prominent band for human ACE2 and for the 2XHA tag at the expected molecular weight of 100 kDa. ACE2 activity measurements were consistent with the immunoblot data in that only COS-7 cells transfected with the 2XHA-hACE2 transgene displayed ACE2 activity. Nonetheless, it is unclear from these studies whether or not addition of the 2XHA tag influenced the observed ACE2 enzyme activity. The 2XHA tag is derived

from an epitope of the influenza hemagglutinin protein, which has been extensively used as a general epitope tag in expression vectors (Field, Nikawa et al. 1988). This epitope tag is commonly used for the labeling and detection of proteins using immunoblotting, and immunostaining techniques (Shevtsova, Malik et al. 2006). Due to their small size, HA tags are unlikely to affect the tagged protein's biochemical properties. Comparative ACE2 activity assay measurements of the transgene with and without the HA tag are required in order to determine the effect of the 2XHA tag on ACE2 activity.

5.15: Generation of podocyte-specific ACE2 transgenic mice

ACE2 transgenic mice were generated with the intent of studying the effects of ACE2 gene manipulations *in vivo.* The human ACE2 transgene was linked to a portion of the nephrin promoter in order to overexpress the human ACE2 gene in the podocyte cells of the glomeruli. The podocyte cell was chosen as the site for overexpression since mouse glomeruli express a relatively low amount of ACE2 as compared to mouse proximal tubules (Velez 2009). ACE2 transgenic mice were successfully identified from wild-type mice by PCR-based genotyping. Immunofluorescence data revealed colocalization of human ACE2 protein with synaptopodin, a podocyte marker, in the glomeruli of the ACE2 transgenic mice. This data suggests that the ACE2 transgenic mice express human ACE2 protein in a podocyte specific manner. Generation of ACE2 transgenic mice will permit future studies focused on the effect of ACE2 overexpression in CKD.

5.16: Conclusions

In the 5/6 Nx mouse model of progressive CKD, ACE2 is down-regulated in the cortex of kidney. 5/6 Nx mice display a mild form of renal injury characterized by urinary albumin excretion, decreased renal function and a modest but not significant increase in systolic blood pressure. Pharmacological inhibition of ACE2 further increases urinary albumin excretion in 5/6 Nx mice via AT_1 receptor-dependent mechanism. Administration of Ang-(1-7) to 5/6 Nx mice did not confer renoprotection nor did it worsen the progression of CKD. The development of ACE2 transgenic mice, which selectively overexpress human ACE2 protein in the glomerular podocyte, will permit future studies focused on the effect of ACE2 overexpression in CKD.

References

Agata and Ura et al. 2006. Olmesartan is an angiotensin II receptor blocker with an inhibitory effect on angiotensin-converting enzyme. Hypertens Res. 29, 865-874.

Benter and Ferrario et al. 1995. Antihypertensive actions of angiotensin-(1-7) in spontaneously hypertensive rats. Am J Physiol. 269, H313-319.

Benter and Yousif et al. 2007. Angiotensin-(1-7) prevents diabetes-induced cardiovascular dysfunction. Am J Physiol Heart Circ Physiol. 292, H666-672.

Benter and Yousif et al. 2008. Angiotensin-(1-7) prevents activation of NADPH oxidase and renal vascular dysfunction in diabetic hypertensive rats. Am J Nephrol. 28, 25-33.

Brinkkoetter and Holtgrefe et al. 2004. Angiotensin II type 1-receptor mediated changes in heparan sulfate proteoglycans in human SV40 transformed podocytes. J Am Soc Nephrol. 15, 33-40.

Brosnihan and Neves et al. 2003. Enhanced renal immunocytochemical expression of ANG-(1-7) and ACE2 during pregnancy. Hypertension. 42, 749-753.

Chappell and Modrall et al. 2004. Novel aspects of the renal renin-angiotensin system: angiotensin-(1-7), ACE2 and blood pressure regulation. Contrib Nephrol. 143, 77-89.

Chappell and Pirro et al. 1998. Metabolism of angiotensin-(1-7) by angiotensin-converting enzyme. Hypertension. 31, 362-367.

Crackower and Sarao et al. 2002. Angiotensin-converting enzyme 2 is an essential regulator of heart function. Nature. 417, 822-828.

Deddish and Marcic et al. 1998. N-domain-specific substrate and C-domain inhibitors of angiotensin-converting enzyme: angiotensin-(1-7) and keto-ACE. Hypertension. 31, 912-917.

Dharmani and Mustafa et al. 2007. Effects of angiotensin 1-7 on the actions of angiotensin II in the renal and mesenteric vasculature of hypertensive and streptozotocin-induced diabetic rats. Eur J Pharmacol. 561, 144-150.

Dilauro and Burns. 2009. Angiotensin-(1-7) and its effects in the kidney. TheScientificWorldJOURNAL. 9, in press.

Donoghue and Hsieh et al. 2000. A novel angiotensin-converting enzyme-related carboxypeptidase (ACE2) converts angiotensin I to angiotensin 1-9. Circ Res. 87, E1-9.

Donoghue and Wakimoto et al. 2003. Heart block, ventricular tachycardia, and sudden death in ACE2 transgenic mice with downregulated connexins. J Mol Cell Cardiol. 35, 1043-1053.

Doobay and Talman et al. 2007. Differential expression of neuronal ACE2 in transgenic mice with overexpression of the brain renin-angiotensin system. Am J Physiol Regul Integr Comp Physiol. 292, R373-381.

Eddy and Falk et al. 1986. Subtotal nephrectomy in the rabbit: a model of chronic hypercalcemia, nephrolithiasis, and obstructive nephropathy. J Lab Clin Med. 107, 508-516.

Epelman and Tang et al. 2008. Detection of soluble angiotensin-converting enzyme 2 in heart failure: insights into the endogenous counter-regulatory pathway of the renin-angiotensin-aldosterone system. J Am Coll Cardiol. 52, 750-754.

Esteban and Heringer-Walther et al. 2009. Angiotensin-(1-7) and the g protein-coupled receptor MAS are key players in renal inflammation. PLoS ONE. 4, e5406.

Field and Nikawa et al. 1988. Purification of a RAS-responsive adenylyl cyclase complex from Saccharomyces cerevisiae by use of an epitope addition method. Mol Cell Biol. 8, 2159-2165.

Gabizon and Goren et al. 1985. Induction of chronic renal failure in the mouse: a new model. Nephron. 40, 349-352.

Gava and Samad-Zadeh et al. 2009. Angiotensin-(1-7) activates a tyrosine phosphatase and inhibits glucose-induced signalling in proximal tubular cells. Nephrol Dial Transplant, doi:10.1093/ndt/gfn736. .

Griffin and Bidani. 2006. Progression of renal disease: renoprotective specificity of renin-angiotensin system blockade. Clin J Am Soc Nephrol. 1, 1054-1065.

Gurley and Allred et al. 2006. Altered blood pressure responses and normal cardiac phenotype in ACE2-null mice. J Clin Invest. 116, 2218-2225.

Hamaguchi and Kim et al. 1998. Activation of glomerular mitogen-activated protein kinases in angiotensin II-mediated hypertension. J Am Soc Nephrol. 9, 372-380.

Hamming and Timens et al. 2004. Tissue distribution of ACE2 protein, the functional receptor for SARS coronavirus. A first step in understanding SARS pathogenesis. J Pathol. 203, 631-637.

Handa and Ferrario et al. 1996. Renal actions of angiotensin-(1-7): in vivo and in vitro studies. Am J Physiol. 270, F141-147.

Hawkins. 2003. Measurement of whole-blood potassium--is it clinically safe? Clin Chem. 49, 2105-2106.

Heller and Kramer et al. 2000. Effect of intrarenal infusion of angiotensin-(1-7) in the dog. Kidney Blood Press Res. 23, 89-94.

Hostetter and Rennke et al. 1982. The case for intrarenal hypertension in the initiation and progression of diabetic and other glomerulopathies. Am J Med. 72, 375-380.

Indridason and Thorsteinsdottir et al. 2007. [Advances in detection, evaluation and management of chronic kidney disease]. Laeknabladid. 93, 201-207.

Joyner and Neves et al. 2007. Temporal-spatial expression of ANG-(1-7) and angiotensin-converting enzyme 2 in the kidney of normal and hypertensive pregnant rats. Am J Physiol Regul Integr Comp Physiol. 293, R169-177.

Khwaja and El Kossi et al. 2007. The management of CKD: a look into the future. Kidney Int. 72, 1316-1323.

Knepper. 1997. Molecular physiology of urinary concentrating mechanism: regulation of aquaporin water channels by vasopressin. Am J Physiol. 272, F3-12.

Kobori and Nangaku et al. 2007. The intrarenal renin-angiotensin system: from physiology to the pathobiology of hypertension and kidney disease. Pharmacol Rev. 59, 251-287.

Kren and Hostetter. 1999. The course of the remnant kidney model in mice. Kidney Int. 56, 333-337.

Lambert and Blackburn et al. 2005. Substrate specificity and novel selective inhibitors of TNF-alpha converting enzyme (TACE) from two-dimensional substrate mapping. Comb Chem High Throughput Screen. 8, 327-339.

Lee and Makaryus et al. 2009. ONTARGET: use of ramipril, telmisartan, or both in patients with high cardiovascular risks. Curr Diab Rep. 9, 185-187.

Lely and Hamming et al. 2004. Renal ACE2 expression in human kidney disease. J Pathol. 204, 587-593.

Levey and Coresh et al. 2003. National Kidney Foundation practice guidelines for chronic kidney disease: evaluation, classification, and stratification. Ann Intern Med. 139, 137-147.

Li and Chappell et al. 1997. Angiotensin-(1-7) augments bradykinin-induced vasodilation by competing with ACE and releasing nitric oxide. Hypertension. 29, 394-400.

Li and Zimpelmann et al. 2005. The role of angiotensin converting enzyme 2 in the generation of angiotensin 1-7 by rat proximal tubules. Am J Physiol Renal Physiol. 288, F353-362.

Ma and Fogo. 2003. Model of robust induction of glomerulosclerosis in mice: importance of genetic background. Kidney Int. 64, 350-355.

Martin and Mellotte et al. 2005. Chronic kidney disease in the elderly; a silent epidemic. Ir Med J. 98, 46-47.

Meyer and Meyer et al. 1985. Picric acid methods greatly overestimate Plasma creatinine in mice: more accurate results with high-performance liquid chromatography. Anal Biochem. 144, 285-290.

Mizuiri and Hemmi et al. 2008. Expression of ACE and ACE2 in individuals with diabetic kidney disease and healthy controls. Am J Kidney Dis. 51, 613-623.

Mundel and Kriz. 1995. Structure and function of podocytes: an update. Anat Embryol (Berl). 192, 385-397.

Navar and Inscho et al. 1996. Paracrine regulation of the renal microcirculation. Physiol Rev. 76, 425-536.

Oudit and Herzenberg et al. 2006. Loss of angiotensin-converting enzyme-2 leads to the late development of angiotensin II-dependent glomerulosclerosis. Am J Pathol. 168, 1808-1820.

Ozono and Wang et al. 1997. Expression of the subtype 2 angiotensin (AT2) receptor protein in rat kidney. Hypertension. 30, 1238-1246.

Paizis and Tikellis et al. 2005. Chronic liver injury in rats and humans upregulates the novel enzyme angiotensin converting enzyme 2. Gut. 54, 1790-1796.

Pendergrass and Averill et al. 2006. Differential expression of nuclear AT1 receptors and angiotensin II within the kidney of the male congenic mRen2.Lewis rat. Am J Physiol Renal Physiol. 290, F1497-1506.

Pendergrass and Pirro et al. 2008. Sex differences in circulating and renal angiotensins of hypertensive mRen(2).Lewis but not normotensive Lewis rats. Am J Physiol Heart Circ Physiol. 295, H10-20.

Pinheiro and Ferreira et al. 2009. Genetic deletion of the angiotensin-(1-7) receptor Mas leads to glomerular hyperfiltration and microalbuminuria. Kidney Int. 75, 1184-1193.

Qi and Breyer. 2009. Measurement of glomerular filtration rate in conscious mice. Methods Mol Biol. 466, 61-72.

Qi and Fujita et al. 2005. Characterization of susceptibility of inbred mouse strains to diabetic nephropathy. Diabetes. 54, 2628-2637.

Reich and Oudit et al. 2008. Decreased glomerular and tubular expression of ACE2 in patients with type 2 diabetes and kidney disease. Kidney Int. 74, 1610-1616.

Remuzzi and Ruggenenti et al. 2002. Chronic renal diseases: renoprotective benefits of renin-angiotensin system inhibition. Ann Intern Med. 136, 604-615.

Ren and Garvin et al. 2002. Vasodilator action of angiotensin-(1-7) on isolated rabbit afferent arterioles. Hypertension. 39, 799-802.

Rentzsch and Todiras et al. 2008. Transgenic angiotensin-converting enzyme 2 overexpression in vessels of SHRSP rats reduces blood pressure and improves endothelial function. Hypertension. 52, 967-973.

Rice and Thomas et al. 2004. Evaluation of angiotensin-converting enzyme (ACE), its homologue ACE2 and neprilysin in angiotensin peptide metabolism. Biochem J. 383, 45-51.

Robertson and Goldschmidt et al. 1986. Long-term renal responses to high dietary protein in dogs with 75% nephrectomy. Kidney Int. 29, 511-519.

Ruiz-Ortega and Esteban et al. 2006. Renal and vascular hypertension-induced inflammation: role of angiotensin II. Curr Opin Nephrol Hypertens. 15, 159-166.

Ruster and Wolf. 2006. Renin-angiotensin-aldosterone system and progression of renal disease. J Am Soc Nephrol. 17, 2985-2991.

Sampaio-Maia and Serrao et al. 2005. Renal dopaminergic system activity in the rat remnant kidney. Nephron Exp Nephrol. 99, e46-55.

Sampaio and Nascimento et al. 2003. Systemic and regional hemodynamic effects of angiotensin-(1-7) in rats. Am J Physiol Heart Circ Physiol. 284, H1985-1994.

Sampaio and Souza dos Santos et al. 2007. Angiotensin-(1-7) through receptor Mas mediates endothelial nitric oxide synthase activation via Akt-dependent pathways. Hypertension. 49, 185-192.

Santos and Brosnihan et al. 1992. Production of angiotensin-(1-7) by human vascular endothelium. Hypertension. 19, II56-61.

Santos and Campagnole-Santos et al. 1994. Characterization of a new angiotensin antagonist selective for angiotensin-(1-7): evidence that the actions of angiotensin-(1-7) are mediated by specific angiotensin receptors. Brain Res Bull. 35, 293-298.

Santos and Simoes e Silva et al. 2003. Angiotensin-(1-7) is an endogenous ligand for the G protein-coupled receptor Mas. Proc Natl Acad Sci U S A. 100, 8258-8263.

Schafer and Lorenz et al. 1995. Role of proteinases in renal hypertrophy and matrix accumulation. Nephrol Dial Transplant. 10, 801-807.

Schlondorff. 2008. Overview of factors contributing to the pathophysiology of progressive renal disease. Kidney Int. 74, 860-866.

Seikaly and Arant et al. 1990. Endogenous angiotensin concentrations in specific intrarenal fluid compartments of the rat. J Clin Invest. 86, 1352-1357.

Shaltout and Westwood et al. 2007. Angiotensin metabolism in renal proximal tubules, urine, and Plasma of sheep: evidence for ACE2-dependent processing of angiotensin II. Am J Physiol Renal Physiol. 292, F82-91.

Shao and He et al. 2008. Chronic angiotensin (1-7) injection accelerates STZ-induced diabetic renal injury. Acta Pharmacol Sin. 29, 829-837.

Shevtsova and Malik et al. 2006. Evaluation of epitope tags for protein detection after in vivo CNS gene transfer. Eur J Neurosci. 23, 1961-1969.

Siragy and Howell et al. 1995. Renal interstitial fluid angiotensin. Modulation by anesthesia, epinephrine, sodium depletion, and renin inhibition. Hypertension. 25, 1021-1024.

Siragy and Inagami et al. 1999. Sustained hypersensitivity to angiotensin II and its mechanism in mice lacking the subtype-2 (AT2) angiotensin receptor. Proc Natl Acad Sci U S A. 96, 6506-6510.

Soldatos and Cooper. 2008. Diabetic nephropathy: important pathophysiologic mechanisms. Diabetes Res Clin Pract. 82 Suppl 1, S75-79.

Soler and Wysocki et al. 2007. ACE2 inhibition worsens glomerular injury in association with increased ACE expression in streptozotocin-induced diabetic mice. Kidney Int. 72, 614-623.

Stephenson and Kenny. 1987. Metabolism of neuropeptides. Hydrolysis of the angiotensins, bradykinin, substance P and oxytocin by pig kidney microvillar membranes. Biochem J. 241, 237-247.

Su and Zimpelmann et al. 2006. Angiotensin-(1-7) inhibits angiotensin II-stimulated phosphorylation of MAP kinases in proximal tubular cells. Kidney Int. 69, 2212-2218.

Taal and Zandi-Nejad et al. 2000. Proinflammatory gene expression and macrophage recruitment in the rat remnant kidney. Kidney Int. 58, 1664-1676.

Takase and Marumo et al. 2005. NF-kappaB-dependent increase in intrarenal angiotensin II induced by proteinuria. Kidney Int. 68, 464-473.

Tikellis and Bialkowski et al. 2008. ACE2 deficiency modifies renoprotection afforded by ACE inhibition in experimental diabetes. Diabetes. 57, 1018-1025.

Tikellis and Cooper et al. 2006. Developmental expression of ACE2 in the SHR kidney: a role in hypertension? Kidney Int. 70, 34-41.

Tikellis and Johnston et al. 2003. Characterization of renal angiotensin-converting enzyme 2 in diabetic nephropathy. Hypertension. 41, 392-397.

Tipnis and Hooper et al. 2000. A human homolog of angiotensin-converting enzyme. Cloning and functional expression as a captopril-insensitive carboxypeptidase. J Biol Chem. 275, 33238-33243.

Trask and Ferrario. 2007. Angiotensin-(1-7): pharmacology and new perspectives in cardiovascular treatments. Cardiovasc Drug Rev. 25, 162-174.

van der Wouden and Ochodnicky et al. 2006. The role of angiotensin(1-7) in renal vasculature of the rat. J Hypertens. 24, 1971-1978.

Velez. 2009. The importance of the intrarenal renin-angiotensin system. Nat Clin Pract Nephrol. 5, 89-100.

Vickers and Hales et al. 2002. Hydrolysis of biological peptides by human angiotensin-converting enzyme-related carboxypeptidase. J Biol Chem. 277, 14838-14843.

Warner and Lew et al. 2005. Angiotensin-converting enzyme 2 (ACE2), but not ACE, is preferentially localized to the apical surface of polarized kidney cells. J Biol Chem. 280, 39353-39362.

Weir. 2009. The renoprotective effects of RAS inhibition: focus on prevention and treatment of chronic kidney disease. Postgrad Med. 121, 96-103.

Wolf. 1998. Link between angiotensin II and TGF-beta in the kidney. Miner Electrolyte Metab. 24, 174-180.

Wong and Oudit et al. 2007. Loss of angiotensin-converting enzyme-2 (Ace2) accelerates diabetic kidney injury. Am J Pathol. 171, 438-451.

Yamamoto and Ohishi et al. 2006. Deletion of angiotensin-converting enzyme 2 accelerates pressure overload-induced cardiac dysfunction by increasing local angiotensin II. Hypertension. 47, 718-726.

Ye and Wysocki et al. 2004. Increased ACE 2 and decreased ACE protein in renal tubules from diabetic mice: a renoprotective combination? Hypertension. 43, 1120-1125.

Ye and Wysocki et al. 2006. Glomerular localization and expression of Angiotensin-converting enzyme 2 and Angiotensin-converting enzyme: implications for albuminuria in diabetes. J Am Soc Nephrol. 17, 3067-3075.

Young and Waitches et al. 1986. Isolation and characterization of a new cellular oncogene encoding a protein with multiple potential transmembrane domains. Cell. 45, 711-719.

Zandi-Nejad and Eddy et al. 2004. Why is proteinuria an ominous biomarker of progressive kidney disease? Kidney Int Suppl.S76-89.

Zhuo and Li. 2007. Novel roles of intracrine angiotensin II and signalling mechanisms in kidney cells. J Renin Angiotensin Aldosterone Syst. 8, 23-33.

Zimpelmann and Burns. 2001. Angiotensin II AT(2) receptors inhibit growth responses in proximal tubule cells. Am J Physiol Renal Physiol. 281, F300-308.

Zimpelmann and Burns. 2009. Angiotensin-(1-7) activates growth-stimulatory pathways in human mesangial cells. Am J Physiol Renal Physiol. 296, F337-346.

Zoja and Abbate et al. 2006. Progression of chronic kidney disease: insights from animal models. Curr Opin Nephrol Hypertens. 15, 250-257.

6.0: Appendix

This section contains a table detailing the antibodies employed for immunoblotting.

Table 5. List of primary and secondary antibodies and their dilutions.

Primary Antibody		**Secondary Antibody**	
Product	Dilution	Product	Dilution
Human ACE2 (R&D Systems, Minneapolis, MN)	1:2000	anti-goat IgG-horseradish peroxidase (HRP) (Jackson ImmunoResearch Laboratories, West Grove, PA)	1:5000
Mouse ACE2 (R&D Systems)	1:2000	anti-goat IgG-HRP (Jackson ImmunoResearch Laboratories)	1:5000
ACE (R&D Systems)	1:2000	anti-goat IgG-HRP (Jackson ImmunoResearch Laboratories)	1:5000
$TGF\beta_1$ (Santa Cruz Biotechnology, Inc., Santa Cruz, CA)	1:1000	anti-mouse IgG-HRP (Amersham, Piscataway, NJ)	1:2000
α-SMA (Sigma-Aldrich, St. Louis, MO)	1:5000	anti-mouse IgG-HRP (Amersham)	1:5000
VCAM-1 (Santa Cruz, Biotechnology)	1:1000	anti-goat IgG-HRP (Jackson ImmunoResearch Laboratories)	1:2000
β-actin (Sigma-Aldrich)	1:5000	anti-mouse IgG-HRP (Amersham)	1:5000
Phospho-p38 MAPK (Cell Signaling, Pickering, ON)	1:1000	anti-rabbit IgG-HRP (Jackson ImmunoResearch Laboratories)	1:2000
p38 MAPK (Total) (Cell Signaling)	1:1000	anti-rabbit IgG-HRP (Jackson ImmunoResearch Laboratories)	1:2000
Phospho-ERK1/2 MAPK (Cell Signaling)	1:1000	anti-rabbit IgG-HRP (Jackson ImmunoResearch Laboratories)	1:2000
ERK1/2 MAPK (Total) (Cell Signaling)	1:1000	anti-rabbit IgG-HRP (Jackson ImmunoResearch Laboratories)	1:2000
HA tag (Clontech Laboratories, Inc., Palo Alto, CA)	1:500	anti-mouse IgG-HRP (Amersham)	1:2000